POLITECNICO DI TORINO

Collegio di Ingegneria Elettronica e Telecomunicazioni

**Corso di Laurea Magistrale
in Ingegneria DET Dipartimento di Elettronica e
Telecomunicazioni**

Tesi di Laurea Magistrale

Controlling Periodicity by Arduino device

Relatore

Prof. Ladislau Matekovits

Candidato

Salehe Yaghoubi

July 2021

Acknowledgements

Abstract

In recent decades, with the emergence and introduction of metamaterial structures, much research has been done to apply these structures in various fields of physics, microwave engineering and optics. Metamaterials are artificial structures with exotic properties, such as negative electric permittivity and magnetic permeability at the same time in a given frequency range, or exhibit frequency stopbands where no signal can propagate. One of the limitations of metamaterial structures is low bandwidth and lack of adjustability. Regulating the structure of the metamaterials, in addition to increase the degree of freedom to control the electromagnetic behavior and scattering of the structure, also solves the problem of low bandwidth.

In this dissertation, a technique to adjust the electromagnetic parameters of a substrate is proposed. In particular, media modulation can be used in controlling the radiation of leaky wave antenna or other exciting applications, such as non-reciprocal metasurfaces, etc. Nowadays, the realization of such dynamic metamaterials is one of the most challenging research areas in the field of metamaterials.

In this design, the "Space-time modulated" media is achieved using a tunable periodic load below a microstrip line. Tunability is obtained by connecting the periodic load of short dipoles below a microstrip line to the ground plan by mean of two diodes. By changing the external bias of the diodes, the effective permeability of the media is controlled.

In this thesis, the goal is to use Model-based design is a process for designing and implementing control systems in which all stages of design, implementation, testing and evaluation of the control system are performed using a software model.

As practical realization concerns, an Arduino Mega 2560 board has been used and programming has been realized using Matlab-Simulink software. Given biasing patterns and their variation in time have been implemented. Verification of the functioning has been checked by controlling a set of 24 diodes. Figures 1 and 2 report a photo of the experimental set-up for all "OFF" and all "ON" cases.
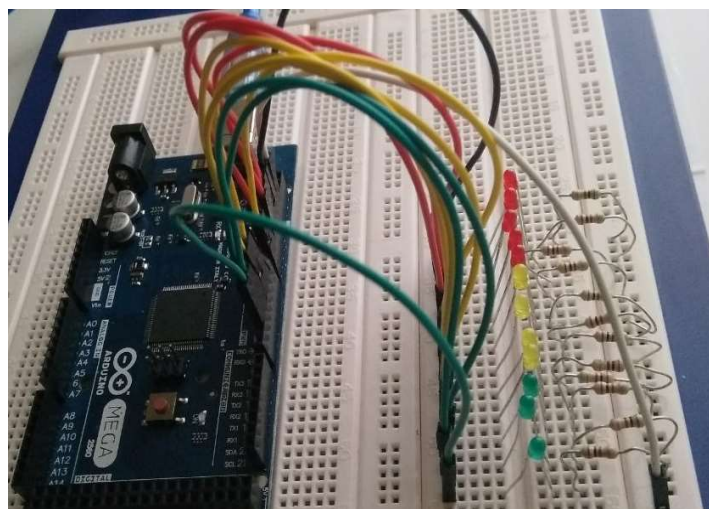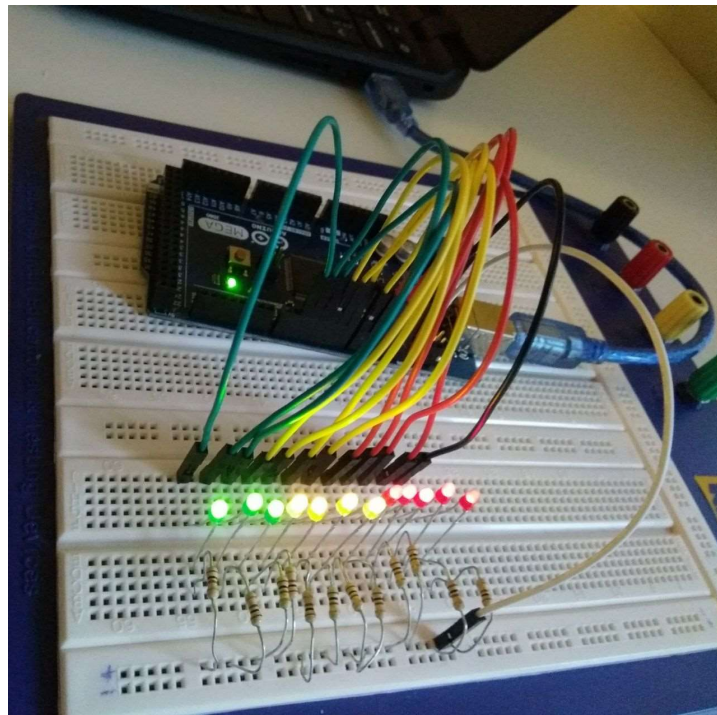
Figure 1: Photograph of the experimental set-up for all "OFF" case

Figure 2: Photograph of the experimental set-up for all "ON" case

Contents

Chapter 1

1 Introduction

1.1 Leaky-wave antenna

In recent years, the idea of rotating the beam without the use of phase shifts with light, simple, flat and mountable antennas on different surfaces have been attracted more attentions. For this purpose, leakage wave antennas that have the ability to propagate the wave from their surface at the desired angle have been proposed. The idea of emitting an electromagnetic wave from a sinus-modulated impedance surface was proposed by Oliner in 1959.

Leakage wave antennas are antennas whose radiation is caused by the leakage of fields from the surface, groove, or aperture on the antenna. In general, leakage wave antennas can be classified into two categories, according to their structure, in uniform, and periodic antennas. T. In uniform wave antennas, the wave phase speed is faster than the speed of light, so the structure can radiate like a moving wave antenna. Wavenumber in the direction of propagation in these structures are complex ($k_z = \beta - j\alpha$).

Periodic leaky wave antennas are slow wave guided waves, meaning that the phase velocity in the guided wave is less than the speed of light in open space. Slow waves are inherently non-diffuse and propagation only in the discontinuity of the helium present in the structure containing them (usually at the antenna power supply and at the end of the antenna termination location) occurs. The number of propagation waves in these waves is a real number in terms of conductor loss and other losses. In this thesis, the periodic structure of leaky wave antenna is discussed.

1.2 Tunable periodic structures

Metamaterials are artificial structures with cells that are smaller than the wavelength of the incident light. These structures are very important because of their ability to control the phase, amplitude and polarization of incident waves. Metamaterials have attracted the attention of many scientists because of their widespread use in the design of antennas, biosensors, invisibility, absorbers, and high-resolution imaging.

Tunable metamaterials are those with the ability to alter their response to an electromagnetic stimulus. Tunability allows adapting the electromagnetic response of metamaterials based on the intended application or effect. In this thesis, we focus on different classes of leaky-wave antennas, based on materials with tunable parameters.

The objective of this study is to present the results obtained by applying the experimental method, using Arduino hardware, to control some active devices like diode within a periodic structure. When we dynamically change the periodicity, it will also influence the material characteristics. Arduino Mega2560, which is used to enable communication and control of connected diodes, was chosen due to its low cost, ease of location. All the proposed tuning scenarios are verified with Arduino board.

1.3 Contribution

Implementation of dynamic control of the change of the periodicity of a 24-bit long sequence by Arduino board. The control program has been implemented in MATLAB, and different configurations have been checked by illuminating LEDs connect to a board. This experimental work has demonstrated the functionality of the developed code, also in case of a time varying control signal. This last configuration can find application in time-modulated periodic structure, a challenging research topic in the today's scientific community.

1.4 Thesis outline

Chapter two of this thesis focuses on the introduction and the concept of leaky wave antennas. In addition, an introduction to metamaterials with different structures, substrate integrated waveguide, and microstrip antenna are provided in this chapter.

The third chapter of this thesis is an introduction and application of different type Arduino. Then the advantages and disadvantages of the Arduino device is provided in this chapter. Moreover, a detailed description of Arduino Mega 2560 is presented. Finally, a short description about the setup and configure of Arduino Hardware to MATLAB are presented.

The design, implementation, and experimental verification of controlling network using Arduino Mega 2560 are described in chapter four. For different scenarios, the effect of different voltages on the diodes' performance are analyzed in detail. In addition, the time-shifting response performance of diodes is investigated.

In the fifth chapter, a summary of the work, the main concepts introduced in each chapter, and the most significant obtained results are presented and commented.
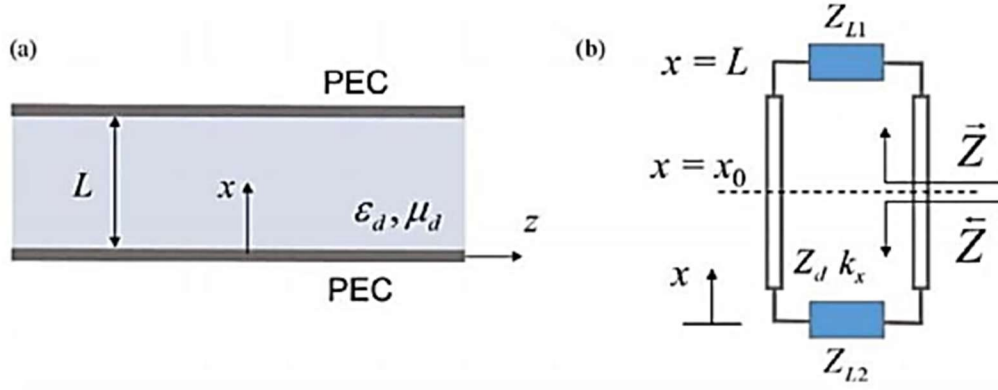
Chapter 2

2 Background

In wave physics, coordinated oscillations in time or space are directly associated with losses in the system. However, it is well known that electrical energy can be gradually lost in the form of radiation in open systems, which indicates the existence of a reduction in the amplitude of the oscillations even when the system is ideal. The examples of this phenomenon can be observed in various fields of physics and engineering, such as radioactive states in quantum mechanics, neutral resonances in electromagnetic holes, and leaky waves in waveguide structures. Despite the seemingly visual concepts of "radiation loss" and "energy leakage", the analysis of wave conduction in open systems is of great importance and theoretically challenging. This project seeks to focus specifically on the fundamental and practical aspects of electromagnetic leaky waves, which is an exciting research topic and is now increasingly recognized in many scientific communities. In recent decades, leaky wave concepts have been successfully used to design radiation systems (leaky wave antennas) [1].

2.1 Concepts and definitions

The early research in the field theory and microwave engineering in the first half of the twentieth century had mostly paid attention to conduction waves in closed systems, such as metal waveguides. In a closed, lossless system, any field distribution satisfying the boundary conditions can be written as a set of effects from specific responses to the source-less problem. The special responses form a discrete, complete, orthogonal spectrum. Each mode obtained in the process has a finite energy (the integral of the quadratic power of the absolute value is limited). In the waveguide structure that is closed in width (in one or two directions), these modes are related to the poles of the Green function. From an engineering point of view, this feature of the Green's function can be interpreted as voltage (or current) in a transmission line along one of the transverse directions of the waveguide. In this network model, the poles are related to the transverse resonance of the network model, which can be easily calculated by using the analytical methods. For example, in a parallel plane waveguide (Figure 2-1), the cross-sectional area can be modeled as follows (Z_L1 and Z_L2 are zeroed for waveguides with PEC plates). The transverse wave number for the source less problem will be obtained by solving the following resonance equation [2]:

$$\vec{Z} + \overleftarrow{Z} = 0 \tag{2-1}$$

Figure 2-1: An example of a closed waveguide structure: a) parallel plane waveguide, b) network transverse model for the application in the transverse resonance method [2]

In waveguide structures without attenuation, eigenmodes are typically described with only real or only imaginary values of the wave number, which represent the propagating wave with a fixed amplitude or the attenuating wave with a fixed phase along the axis of the waveguide. By considering material losses, these eigenmodes are complex according to the absorption and degradation of the corresponding modal. Conversely, open systems can support complex eigenmodes, even in the non-loss mode, due to radiation losses, as described below.

Open waveguides, as radiation systems, were first studied by Hansen in the late 1930s, who proposed an antenna with a longitudinal slit next to a rectangular waveguide. However, the early development of these concepts was delayed due to a limited understanding of the physical mechanism of leaky waves. Soon, a leaky waveguide mode with a complex wave number and constant attenuation (due to radiation losses) was recognized. In some cases, this fact is related to seemingly non-physical results. The longitudinal coherence may correspond to an increase in wave amplitude across the transverse plane to infinity. For example, consider the following structure (Figure 2-2), which has a longitudinal direction of z (parallel to the waveguide axis) and a transverse direction of X, where the upper part of the wave-conducting structures is fully or partially open, so that part of the energy can leak in the semi-infinite high region.

Leak fields from the aperture have a complex longitudinal (horizontal) wave number kz ($kz = \beta - j\alpha$ with time contract e^{jwt}), where the real values α and β are phase constant and attenuation, respectively. The fields above the waveguide aperture are specified by a transverse (vertical) wave number through the HelmHoltz equation:

$$k_0 = \pm\sqrt{k_0^2 - k_z^2} = \beta_x - j\alpha_x \qquad (2\text{-}2)$$

For a mode that carries power in the positive direction z, we have $\alpha > 0$. Further, we have $\beta > 0$ for a wave moving in the +Z direction. Therefore, it is necessary to have $\alpha_x < 0$, which means that the leakage mode fields increase exponentially in the transverse direction (X direction). This result surprised early researchers in leaky wave theory. Thus, there seemed to be some doubt about the leak mode due to this non-physical behavior. This issue was not resolved until the late 1950s regarding the deeper theoretical understanding and physical insight provided by the works of Markovich and Evilin.

4

Figure 2-2: Leaky wave radiation from open waveguide. The curves on the *xz* plane display the distribution of the electric field over time as the wave conducts in the open system and does not leak. The diagram on the *yz* plane shows the exponential decrease of the electric field amplitude in the longitudinal direction of the waveguide [2]

It should be noted that the spectrum of eigenmodes is completely discrete in closed systems and continuous in open systems, which is determined by the branch cut of Equation (2-2) . For a waveguide structure that is open on one side, Figure 2-3 shows the complex plane of the longitudinal wave number with the general selection of the branch cut. An appropriate spectral solution to the electromagnetic problem is to excite the integral source around the upper Riemannian sheet, which corresponds to waves that decrease in the transverse direction in infinite. However, as shown in Figure 1.3, polar singularities may also be present in the lower Riemannian sheet, and consequently, the methods are called non-suitable responses to the field equations, which are related to leakage modes. Despite the lack of being suitable spectral responses, they can accurately explain the electromagnetic field in finite regions.

Figure 2-3: Complex plane of the longitudinal wavenumber for an open waveguide on one side; Green lines represent the branch cut [2].

The angle of radiation in the leaky wave antenna in the general form is obtained by the following relation:

$$\theta = tan^{-1}\left(\frac{Re[k_x]}{Re[k_z]}\right) \hspace{3cm} (2\text{-}3)$$

If a is small and the antenna length is long, the relation can be approximated by the following relation:

$$\theta = cos^{-1}\left(\frac{\beta}{k_0}\right) \hspace{3cm} (2\text{-}4)$$

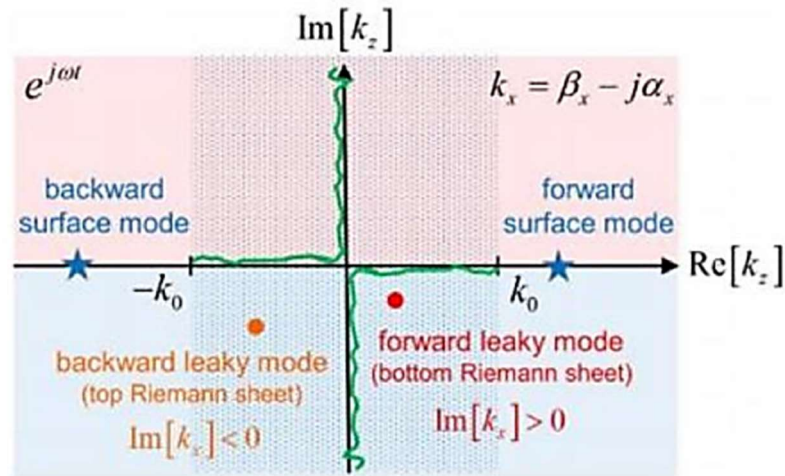For a forward wave, the amplitude of the leakage mode increases exponentially as expected in the vertical (transverse) direction X. However, this issue is only acceptable in the spatial region $x < z * \tan\theta$ for a source placed at $z = 0$, meaning that the leaky wave has always a limited amplitude and becomes a valid representation of the radiation field. For a forward wave, a decrease in amplitude of the electric field along the positive Z axis directly reflects the exponential growth of the field along the X direction. On the other hand, the electric field around the antenna is limited as shown in Figure 1.2.

Equation (2-4) shows that the radiation of a leaky wave is supported along the waveguide only by a fast wave (i.e. waves with a phase velocity faster than the speed of light) because Equation (2-4) gives a real angle only if $|\beta| < k_0$. In other words, by having a fast wave, the leaky wave can be coupled to a plate wave in outer space; otherwise, this issue will not be possible (in the slow wave mode).

The next section discusses the fundamental differences between closed and open electromagnetic systems and the interpretation of leaky waves as source less modal responses within waveguides. It is worth noting that in microwave frequencies, closed systems are defined using impermeable metal walls, while electromagnetic nanostructures are open in the optical range, as materials lose their permittivity properties at high frequencies and ideal conductors are not available in optics. In the next section, we will review the general principles and recent developments in the field of leaky wave antennas in microwave frequencies.

2.1   leaky-wave antenna

2.1.1   Basic characteristics

Leaky wave has been constantly evolving since the 1950s, and microwave leaky antennas are popular due to their attractive features, especially the ability to realize modern antennas without the need for complex power grids for fuzzy arrays. The advent of supernatural materials or synthetic materials with unusual electromagnetic properties has made researchers over the past 15 years to study leaky wave antennas, as their new properties can overcome the limitations of conventional designs.

The motion of the wave traveling along the antenna achieves an effective surface that radiates energy to the remote area. The radiation pattern can be obtained by converting the Fourier transform from the aperture fields. The complex wave number of the leaky wave directly

determines the main characteristics of the radiation pattern such as the main beam angle, beam width, and the surface of the lateral lobes. In this way, a large leakage coefficient means low effective level and consequently, wide beam width. For a uniform one-dimensional antenna, the half-power beam width is calculated approximately by the equation (2-5). If the leakage coefficient is small, it can reduce the surface area of the lateral lobes by gradually reducing the aperture.

$$BW = 2\csc(\theta)\alpha/k_0 \qquad\qquad (2\text{-}5)$$

Generally, the ability to sweep the main beam by changing the frequency, considering the constant dependence of the phase on the frequency, is regarded as one of the features of the leaky wave antenna. For many leaky wave antennas, radiation in the broadside direction and continuous sweep with constant beam width are a challenge that has been one of the important research topics in recent years. Different categories of leaky wave show different characteristics of beam sweeps that are related to different geometric structures. To achieve a constant beam width for high bandwidth, the slope of the scatter diagram needs to be low.

2.1.2 Classification

Generally, classifying leaky antennas in different classes is a challenging task, given the wide range of different designs provided in the last sixty years. According to numerous articles and books in this field, leaky wave antennas are categorized depending on the uniform or alternating geometry of the structure [1]. The direction of the traveling wave in the structure is another important distinction between antennas. Depending on whether the traveling wave propagates in one or two directions in the structure, leaky wave antennas are divided into two categories of one-dimensional or two-dimensional. Figure 2-4 illustrates examples of one-dimensional and two-dimensional antennas.
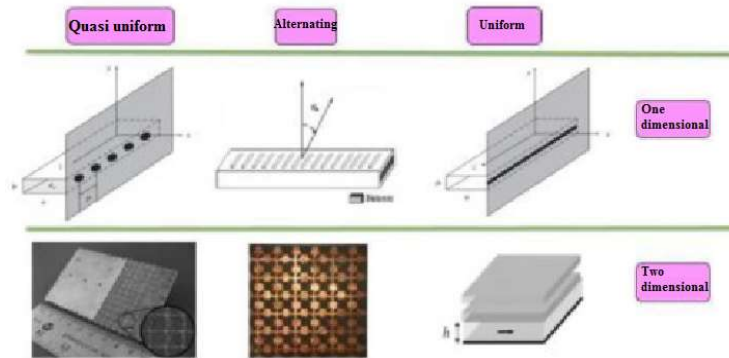

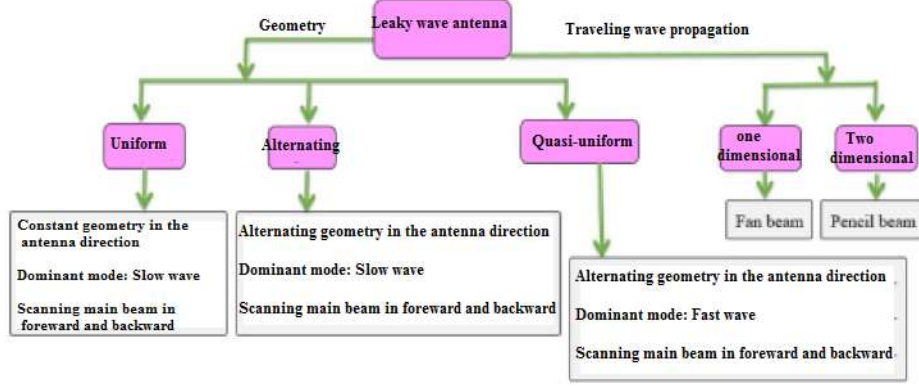**Figure 2-4: Samples of leaky wave antenna [1]**

Figure 2-5: Classifying leaky wave antennas [1]

The uniform antenna has the same geometry along the antenna, and the fast wave is its predominant mode. Further, a uniform antenna can only sweep the beam in the forward direction. Examples of these antennas include a rectangular waveguide antenna with a continuous slit (one-dimensional) and a dielectric leaky wave antenna (two-dimensional) (Figure 2-4). On the other hand, a certain geometry with periodicity (comparable to wavelength) is repeated in alternating antennas, the predominant mode of which is slow wave, and it will not radiate even if the structure is open, as discussed below. Examples of this mode are the aperture array antenna in one-dimensional mode and the microstrip antenna consisting of transmission lines in two-dimensional mode (Figure 2-4). Note that there is an periodic structure quasi-uniform antenna, which is much smaller compared to the wavelength and the predominant mode in these structures is fast wave. Although there is other harmonics, radiation is related to the dominant mode. A well-known example of this type of leaky wave antenna is the antenna consisting of metamaterial transmission lines, which will be examined below. Figure 2-5 shows examples of these categories.

2.1.3   Radiation in periodic antennas

According to Bloch's theorem, it can be proved that the fields of periodic structure can be written as a sum of infinite harmonic series. Each harmonic has its own longitudinal wave number. On the other hand, it can be proved that the wave numbers of harmonics are periodic with the periodicity of the structure.

$$E(x, y, z) = \sum_{n=-\infty}^{\infty} A_n(x, y) e^{-jk_{z,n}z} , k_{z,n} = k_{z,0} + \frac{2\pi n}{p} \tag{2-6}$$

where p represents the period of rotation, n indicates the harmonic number, k_{z0} shows zero harmonic, and k_{z0} displays approximately a structure in which the effects of periodicity tend to zero. In the following, we first examine the harmonic $n = -1$. The wave number related to this harmonic is smaller than k_0, which indicates a fast wave. Thus, it has the ability to couple with the radiation mode. The parameter $k_{z,n}$ takes a value greater than k_0 ($k_{zn} > k_0$) for values $n > -1$, which corresponds to a forward slow wave, and takes a value smaller than k_0 for values $n < -1$ ($k_{zn} < k_0$), which is related to the backward slow wave. Therefore, only the harmonic $n = -1$ in periodic structures can radiate leaky wave.

2.1.4 Broadside radiation challenge

As mentioned, broadside radiation is one of the main challenges in the design of leaky wave antennas. First, we investigate the cause of this inability in the leaky wave antenna and then, introduce a solution to solve this problem. The orbital model shown in Figure 2-6 shows an periodic antenna with p-period. In this model, the antenna is modeled with the transmission line and each of the discontinuities or slits on the antenna is modeled through impedance. When the antenna is stimulated at the frequency of the broadside radiation, each of the radiant elements on the antenna is excited with the same phase, and as a result, the traveling wave becomes a standing wave [3].

At this time, short circuit boundary conditions are created for each of the elements and the elements lose the ability to radiate. Furthermore, impedance becomes fully reactive for an antenna with infinite cells. Therefore, we expect the lack of impedance matching at this frequency, which is called open stop band. The viewpoint of the transmission line has proved that the use of only one radiation mechanism creates the stop band. So far, two radiation mechanisms have been used to solve this problem. To better understand this issue, consider the circuit model of a transmission line consisting of an inductor and series resistors and capacitors, as well as parallel conductors.

Figure 2-7-a shows the scatter diagram in the case of adding a series capacitor and a parallel inductor to the transmission line. As observed, the graph consists of two blue curves, where ω_{se} and ω_{sc} represent the parallel resonance frequency and the series of parallel and series resonators in the orbital model, respectively.
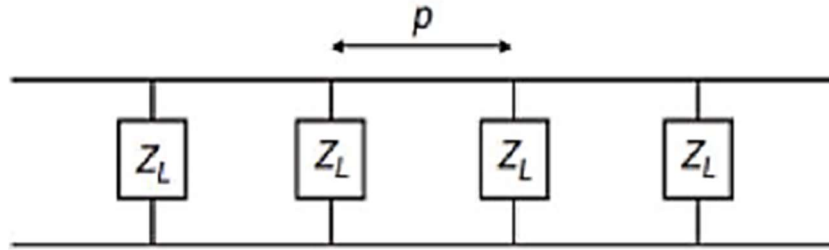

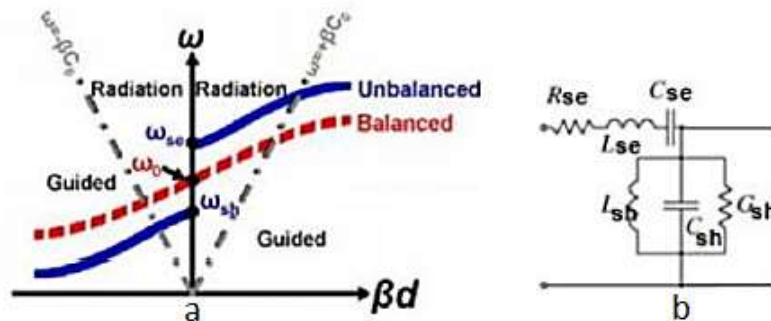**Figure 2-6: The transmission line model for the periodic antenna**

Figure 2-7: Antenna with two radiation mechanisms: a) scatter diagram, b) circuit model [2]

If the series and parallel resonance frequencies are equal, the closed stop band problem is solved, and the scatter diagram is in balance mode. In this way, the group speed will not be zero at the broadside frequency.
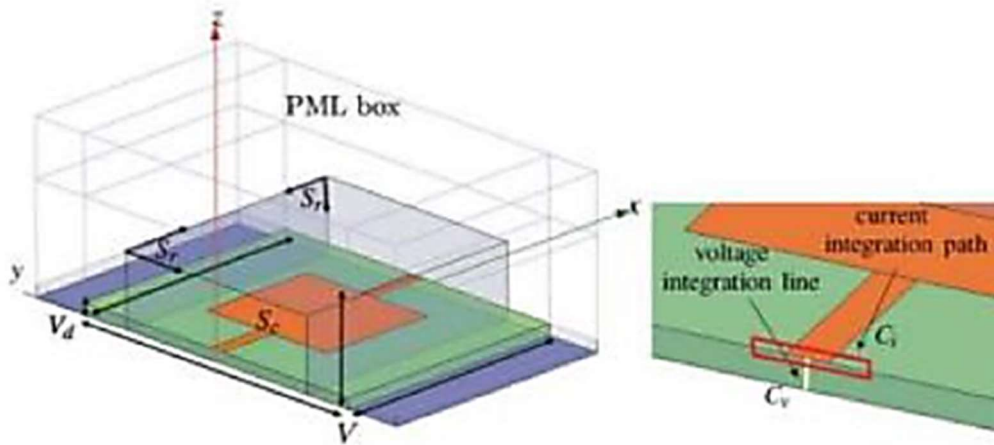
To provide proper radiation in the broadside direction, another condition is required in addition to equal resonance frequencies. If the quality coefficient (Q) of the two resonators is not equal, the radiation pattern

will not be at its optimal state. In addition, equal quality coefficient for two resonators provides constant leakage coefficient and appropriate impedance matching. Therefore, it is necessary to provide this condition in the designs to have the same orientation in the sweeping and to match an appropriate impedance.

2.1.5 Analysis of eigenmodes of leaky wave antenna

In this analysis, which is performed by simulation software, by applying boundary conditions to the initial cell of the periodic structure that models the infinite structure, it is possible to obtain eigenmodes of structure and distribution of electric field, magnetic field, and electric current, and then, calculate the parameters of the cell orbital model through following equations. Figure 2-8 shows an example of the structure for a single cell. The coupling effect of the elements is also addressed by considering the boundary condition of the ideal magnetic walls in the radiation surfaces.

Figure 2-8: Simulation settings for parameter extraction [2]-Left) Periodic boundary conditions on both sides of the cell; Right) Voltage and current integration paths

First, we calculate the energy and power using the fields obtained from the simulation:

$$BW = W_e + W_m = 2W_m = 2W_e = 2\left(\frac{1}{4}\right)\mu_0 \int_V \vec{H}.\vec{H}^* dv \qquad (2\text{-}7)$$

$$P_r = \frac{1}{2}\int_{S_r} \vec{E}.\vec{H}^*.d\vec{s} \qquad (2\text{-}8)$$

$$P_d = \frac{1}{2}\int_{V_d} \vec{E}.\vec{J}^*.dv \qquad (2\text{-}9)$$

$$P_c = \frac{R_s}{2}\int_{S_c} \overrightarrow{H_{tan}}.\overrightarrow{H_{tan}}^*.ds \qquad (2\text{-}10)$$

where the indices e and m represent electrical and magnetic values, respectively. The indices r, d, and c indicate radiative, dielectric, and conductor losses, respectively. The vectors E, H, and J represent the electric and magnetic fields and the density of the conducting current, respectively. The quality factor of a single cell is calculated as follows.

$$Q = \frac{\omega_0 W}{P_r + P_d + P_c} = \frac{\omega_0 W}{P}$$

(2-11)

By assuming the symmetry of the structure in the transverse direction and using even and odd analysis (Figure 2-9), we calculate the series current and parallel voltage.

$$I_{se} = \oint_{c_i} \overrightarrow{H_{PEC}} . d\vec{l} \quad (V_{se} = 0)$$

(2-12)

$$V_{sh} = \oint_{c_v} \overrightarrow{H_{PMC}} . d\vec{l} \quad (I_{sh} = 0)$$

(2-13)

Figure 2-9: Orbital model equivalent to the primary cell with respect to symmetry [2] Left) Electric wall for series mode Right) Magnetic wall for parallel mode

In this way, the reactive parameters of the orbital model are obtained according to the stored electrical and magnetic energy and the current or voltage related to the desired mode, and the resistance parameters are calculated according to the dissipated power.

For series resonators:

$$C = C_{sh} = \frac{4W_e}{|V_{sh}|^2}, L_{sh} = \frac{1}{\omega_{sh}^2 C_{sh}}$$

$$G_r = \frac{2P_r}{|V_{sh}|^2}, G_d = \frac{2P_d}{|V_{sh}|^2}, G_c = \frac{2P_c}{|V_{sh}|^2}$$

(2-14)

$$G = G_r + G_d + G_c$$

For parallel resonators:

$$L = L_{se} = \frac{4W_m}{|L_{se}|^2}, C_{se} = \frac{1}{\omega_{se}^2 L_{se}}$$

$$R_r = \frac{2P_r}{|I_{se}|^2}, G_d = \frac{2P_d}{|I_{se}|^2}, G_c = \frac{2P_c}{|I_{se}|^2}$$

(2-15)

$$R = R_r + R_d + R_c$$

2.1.6 Analysis of dispersion matrix parameters of leaky wave antenna

In this analysis, we first simulate several cells and obtain S parameters to calculate the ABCD matrix for N cells. Given that the cells are identical and the ABCD matrix for N cells is equal to the multiplication of the ABCD matrix of each cell, the matrix can be calculated by calculating the Nth root of the total matrix for a cell.

On the other hand, the ABCD matrix for the orbital model of a series impedance and a parallel admittance is calculated as follows. Therefore, the parameters of the orbital model can be calculated through the following relations:

Figure 2-10: Orbital model

First, it is possible to obtain the series and parallel resonance frequencies by using the imaginary part of impedance and admittance, which are equal to B and C arrays, respectively.

$$Im(Z_{se})|_{\omega_{se}} = 0, Im(Y_{sh})|_{\omega_{sh}} = 0 \tag{2-16}$$

Given that each resonator has a real value at the impedance resonance frequency, we calculate the values of R and G, and finally, calculate the reactive parameters of the orbital model.

$$G = Re(Y_{sh})|_{\omega_{sh}} R = Re(Z_{se})|_{\omega_{se}}$$

$$C_{sh} = \frac{1}{2}\frac{\partial}{\partial\omega}Im(Y_{sh})|_{\omega_{sh}}, \qquad L_{se} = \frac{1}{2}\frac{\partial}{\partial\omega}Im(Z_{se})|_{\omega_{se}} \tag{2-17}$$

$$L_{sh} = \frac{1}{\omega_{sh}^2 C_{sh}}, \qquad C_{se} = \frac{1}{\omega_{se}^2 L_{se}}$$

2.2 Background about meta material and periodic structure

In recent decades, advances have been made in the field of wireless telecommunications. Antennas, as one of the main components of wireless telecommunication systems, have a direct impact on the performance and limitations of these systems. This dissertation aims to design and analyze the structure of a leaky wave antenna, in which the ability of the antenna beam to rotate in the forward and backward regions has been performed by using the metamaterial

structure. The dissertation focuses on making the leaky wave antenna adjustable using magnetic material and bias perpendicular to the structure. By making the structure adjustable, it is possible to continuously scan the entire spatial (one dimensional) by changing the external magnetic field at a constant frequency. This issue can be used in telecommunication systems that scan the space at a constant frequency or limited bandwidth.

The rotation of radiation beam in leaky wave antennas is performed with frequency change or an external lever. Virtually, any factor that changes the phase constant relative to the free space wave number changes the direction of antenna propagation. In many of these antennas, the beam is rotated by changing the frequency, which is challenged by providing an RF source and limiting performance in narrowband and constant frequency applications.

So far, several methods, including the use of pin-diode, varactor diode [4], MEMS switch [5], and magnetic excitation have been proposed for rotating the beam at a constant frequency.

Considering the positive phase constant in conventional leaky wave antennas, space scanning can only be performed in the direct direction (angle 0 to 90 degrees) and do not cover the backward area (angle 0-10 degrees). The main solution to this problem is to use metamaterial structures because of the existence of two left-handed and right-handed ranges, so that the wave can fully scan the entire space.

The following is a list of the recent research and development in the field of leaky wave antennas, which is still ongoing:
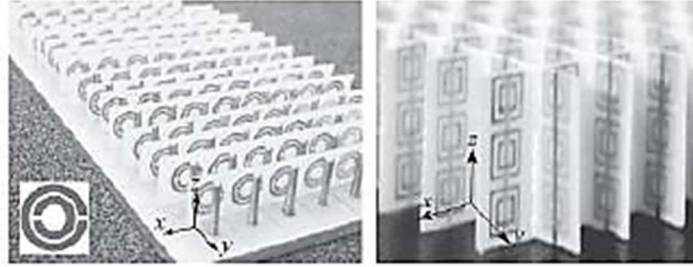
Designing a leaky wave antenna array with power recovery supply network to improve radiation efficiency [6]. Using graphene in design of two-dimensional adjustable leaky wave antenna in terahertz band [7]. Designing a leaky wave antenna as a substrate integrated waveguide with circular polarization in a wide range [8]. Designing a leaky wave antenna as a three-layer substrate integrated waveguide using left-handed and right-handed composite line [9].

2.2.1 Metamaterials

Metamaterials, which are synthetic structures with abnormal electromagnetic properties, have received much attention in recent years. These materials are realized by designing the structure in such a way that simultaneously negative magnetic permeability (μ) and electrical permittivity (ε) are created in a frequency range. In order to get a homogeneous structure of the metamaterial, the unit cell length (p) should be much smaller than the guided wavelength (λ_g) in the structure ($p \leq \lambda_g/4$) [10]. In this regard, the left-handed characteristic of wave and the non-compliance of the directions of phase velocity and group velocity are among the unusual behaviors of metamaterial structure.

The history of metamaterials began in 1967 by Veselago with the theory of the possibility of a material with a simultaneously negative electrical permittivity (ε) and magnetic permeability (μ) [11]. Veselago concluded that if there were left-handed material, the electric field, magnetic field, and the direction vector of wave propagation would not follow the right-hand law like ordinary materials. Moreover, the opposite of Snell's law, the Doppler effect, and Vavilov-

Cherenkov radiation would occur. Smith et al. (2000) conducted experiments on Veselago research [12], [13] and obtained the first left-handed structure with simultaneously negative permeability and permittivity near the structure's resonant frequency, by using Split Ring Resonator (SRR) and metal rods (Figure 2-11). The features of this type of metamaterial structure are the presence of left-handed property near the resonant frequency, large dimensions, high losses, and low bandwidth. A more practical way to realize metamaterials is to use the left-hand transmission line to accomplish a non-resonant structure.

Figure 2-11: The first left-handed structures, the combination of parallel rods array and SRR array [10]

2.2.2 Metamaterials application

Research conducted in the field of metamaterials in recent years has led to the design and construction of practical structures in various fields, including microwave engineering and telecommunications, which will be discussed briefly in the following.

The number of design parameters in the composite transmission line (C_L, L_L, C_R, L_R) is more than that of the right-handed transmission line (C_R, L_R). For this reason, the degree of freedom in designing the structure of metamaterials is greater. This advantage has been used in designing different metamaterial-based microwave devices to improve bandwidth, duplicating, and downsizing. Figure 2-12display some examples of recent research in this field.

- Designing and fabricating a downsized metamaterial absorber with cell dimensions of $0.0036\lambda^2$ (75% downsizing) in the UHF band [14].
- Designing microstrip compact double-band duplexer using composite line SR and CSRR [15].
- Designing compact and broadband antenna (bandwidth 109.1%) using left-handed and right-handed combined line and modified ground plate [16].

Figure 2-12: Composite line application (a) absorbent compression, (b) duplexer duplicating, (c) antenna broad banding

Another application of metamaterials is the design of the zeroth-order resonant structure, which is based on the existence of a zero-propagation constant at the left-handed and right-handed composite line passing frequency [17]. In general, an intensifier is created when a short- or open-circuit occurs at the end of the transmission line. Concerning the right-handed line intensifier with physical length l, intensification occurs when:

$$\beta l = \frac{2\pi l}{\lambda_g} = n\pi \qquad n = 1,2,3, \dots \qquad (2\text{-}18)$$

Given that the phase constant can be positive, negative or zero in the balanced composite line, we have $n = 0, \pm 1, \pm 2, \dots$ in the above relation (Figure 2-13).

Figure 2-13: a) Resonance modes in an open-circuit end composite line intensifier (b) propagation constant change curve in terms of frequency in a balanced composite line

In the composite line, the phase constant becomes zero at a non-zero frequency (passage frequency) and intensification occurs independent of physical length. This feature is used in the design of zeroth-order resonators to downsize intensifiers.

2.2.3 Tunable Metamaterials

Regarding the development of telecommunication systems and the complexity of their operation, the design of adjustable devices is of great importance. Adjusting the structure of the metamaterials can solve the problem of low bandwidth, in addition to increasing the degree of freedom to control the magnetic electrode behavior of the structure by an external lever. There are various methods for realizing adjustable circuits and devices, the most common of which are the use of semiconductor elements (such as varactor diodes) [18], micro-electromechanical switches (MEMS) [19], ferroelectric material [20], and ferromagnetic material [21]. Each of the adjustable methods has its own advantages and limitations, which will be briefly discussed in the following.

Semiconductor diodes have low weight, low cost, and simple bias, while nonlinear effects, transmission losses, and interfering noise are among the disadvantages of this method. The MEMS switch is highly linear relative to the varactor diodes while the operation of the switch and its response are slow and discrete and are vulnerable relative to environmental conditions such as temperature and vibration. The ferroelectric material has high adjustability and fast response, but high dielectric loss and low-quality factor. Ferromagnetic adjustable devices are capable of withstanding high power compared to MEMS and varactor. The quality factor and capability of high adjustability are other features of this method. To bias magnetic material, a permanent magnet or coil with the carrier current is usually used which can sometimes cause problems such as enlarging the dimensions of the device [22].

In general, magnetic material is used in designing the structure of metamaterials for the following reasons:

1. The effective permeability of ferrite in a frequency range is negative.
2. By changing the external bias field, the effective permeability of ferrite and as a result, the electromagnetic behaviour of the structure is adjusted.

2.2.4 Orbital analysis for periodic structure

In the case of applying the periodicity condition to the orbital model of the structure, it is possible to obtain the leakage coefficient and the propagation constant for the antenna according to the ABCD matrix of a cell. On the other hand, the wave propagated inside the periodic structure is seemed to be propagated in the waveguide structure with specific impedance, which is called Bloch's impedance.

$$\begin{bmatrix} V_n \\ I_n \end{bmatrix} = \begin{bmatrix} A & B \\ C & D \end{bmatrix} \begin{bmatrix} V_{n+1} \\ I_{n+1} \end{bmatrix} \tag{2-19}$$

$$V_{n+1} = V_n e^{-\gamma d}, \qquad I_{n+1} = I_n e^{-\gamma d} \tag{2-20}$$

$$Z_B = Z_0 \frac{V_{n+1}}{I_{n+1}} \tag{2-21}$$

Figure 2-14: ABCD matrix of a cell

Proof:

Calculation of propagation and attenuation constants in terms of ABCD matrix

$$\begin{bmatrix} A - e^{\gamma d} & B \\ C & D - e^{\gamma d} \end{bmatrix}\begin{bmatrix} V_{n+1} \\ I_{n+1} \end{bmatrix} = 0 \tag{2-22}$$

$$\gamma = \alpha + j\beta \tag{2-23}$$

$$AD + e^{2\gamma d} - (A + D)e^{\gamma d} - BC = 0 \tag{2-24}$$

$$Cosh\,\gamma d = \frac{A + D}{2} \tag{2-25}$$

Calculation of Bloch impedance in terms of ABCD matrix

$$Z_B = Z_0 \frac{V_{n+1}}{I_{n+1}} \left((A - e^{\gamma d})V_{n+1} + BI_{n+1} = 0 \right) \tag{2-26}$$

$$Z_B = \frac{-BZ_0}{A - e^{\gamma d}} \tag{2-27}$$

$$(e^{\gamma d}) = \frac{1}{2}(A + D \pm \sqrt{(A + D)^2 - 4}) \tag{2-28}$$

$$Z_B^{\pm} = \frac{-2BZ_0}{A - D \pm \sqrt{(A + D)^2 - 4}} \tag{2-29}$$

2.3   Substrate integrated waveguide

The substrate integrated waveguide is a type of transmission line, which has been highly considered by researchers in designing and manufacturing various microwave devices such as filter, power divider, coupler, antenna. This system combines the advantages of the rectangular waveguide structure, such as low losses and high-quality coefficient, with features of plate transmission line structure such as compatibility with integrated and microwave circuits, simplicity of impedance matching, simplicity of construction, and low cost.

The substrate integrated waveguide is a type of rectangular waveguide that consists of two metal plates separated by a dielectric substrate, and the lateral walls are formed by a row of holes with via walls. Figure 2-15 shows a substrate integrated waveguide where w represents the distance between two via rows, d indicates the via diameter, and s shows the center-to-center distance of two consecutive via. The size s should be small enough to reduce losses

17

between two adjacent via. In this regard, to reduce losses and provide the optimal performance of the substrate integrated waveguide, it is better to consider the following two conditions [23]:
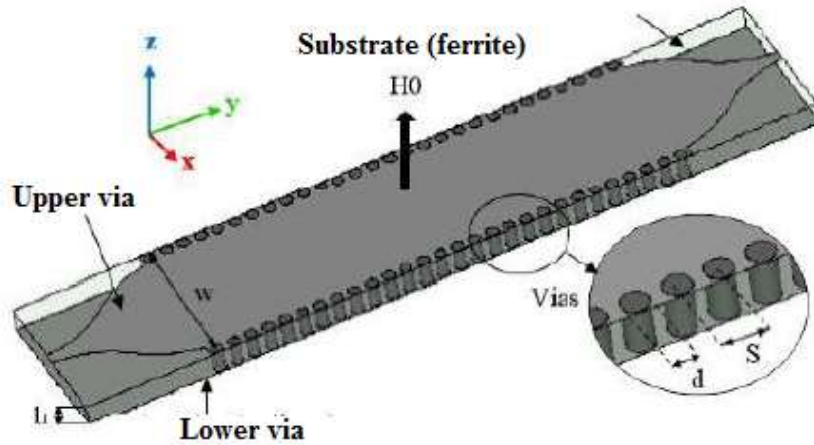
$$d < \frac{\lambda_g}{5} \tag{2-30}$$

$$s \leq 2d \tag{2-31}$$

By considering appropriate values for S and d, the losses due to the distance between via can be ignored and the equations for the electromagnetic fields can be solved similar to the rectangular waveguide.
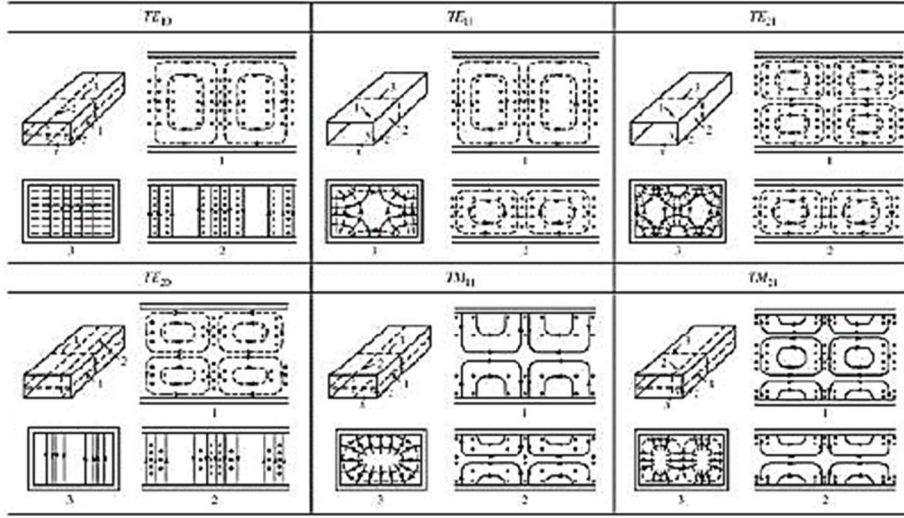
The results of experimental and simulation experiments have shown that the effective width of the substrate integrated waveguide is not equal to the distance between the two side walls consisting of via (w) and is obtained from the following relation:

$$w_{off} = w - 1.08 \frac{d^2}{s} + 0.1 \frac{d^2}{w} \tag{2-32}$$

Figure 2-15: Substrate integrated waveguide with bias perpendicular to the structure

In the rectangular waveguide, TE and TM modes can be propagated, while only TE_{m0} modes are propagated in the substrate integrated waveguide [24]. The reason for this difference is that the side wall is composed of via and is not continuous in the substrate integrated waveguide; hence, the longitudinal surface current required to propagate TM and TE_{m0} modes with $n \neq 0$ is interrupted and the substrate integrated waveguide cannot propagate these modes. In TE_{m0} modes, the current distribution is not interrupted by via, and as a result, these modes can be propagated. Figure 2-16 illustrates the shape of the fields of several different modes of rectangular waveguide.

Figure 2-16: The field lines of different modes in a rectangular waveguide (electric field is marked with a straight line while the magnetic field is marked with a dashed line.)

2.3.1 The structure of the periodic leaky wave antenna

In the metamaterial substrate integrated waveguide, the structure is used as a leaky wave antenna in the frequency range where the leakage wave condition $|\beta| < K_0$ is met. Next, we theoretically determine the leakage wave region in the periodic substrate integrated waveguide.

In a periodic leaky wave antenna, there are an infinite number of harmonics, which are characterized by a phase constant β_n (corresponding to the nth harmonic) and related by the following relation:

$$\beta_n = \beta_0 + \frac{2\pi n}{p} \tag{2-33}$$

where p represents the periodicity of the structure and β_0 is the main harmonic, which is the same as the phase constant of the waveguide dominant mode without interference. It is worth mentioning that the small size of the slits has no significant effect on the electromagnetic behavior of the structure.

On the other hand, the parameter β_n can have different values so that the wave is slow or fast and is in the foreward or backward region. Usually, the harmonic $n = -1$ is selected in a practical leaky wave antenna with optimal physical dimensions:

$$|\beta_{-1}| = \left| \beta_0 - \frac{2\pi}{P} \right| < k_0 \tag{2-34}$$

Therefore, the parameters p and β_0 are considered so that the above condition is met. To determine the frequency range of the leaky wave ($|\beta_{-1}| < k_0$) for a waveguide-based leaky wave antenna (SIW) and to ensure that subsequent harmonics (usually β_{-2}) do not interfere and cause grating lobes, the scattering curve is drawn for several harmonics.

The phase constant of a rectangular waveguide is obtained by the following equation:

$$\beta = \sqrt{k^2 - k_c^2} \tag{2-35}$$

where K_c is the cut-off wave number and is calculated from the following equation:

$$k_c = \sqrt{(\frac{m\pi}{w_{off}})^2 + (\frac{n\pi}{b})^2} = \underline{TE_{m0}} \ k_c = \frac{m\pi}{w_{off}} \qquad (2\text{-}36)$$

As a result, the phase constant for the TE_{m0} mode propagated in the substrate integrated waveguide can be calculated as follows:
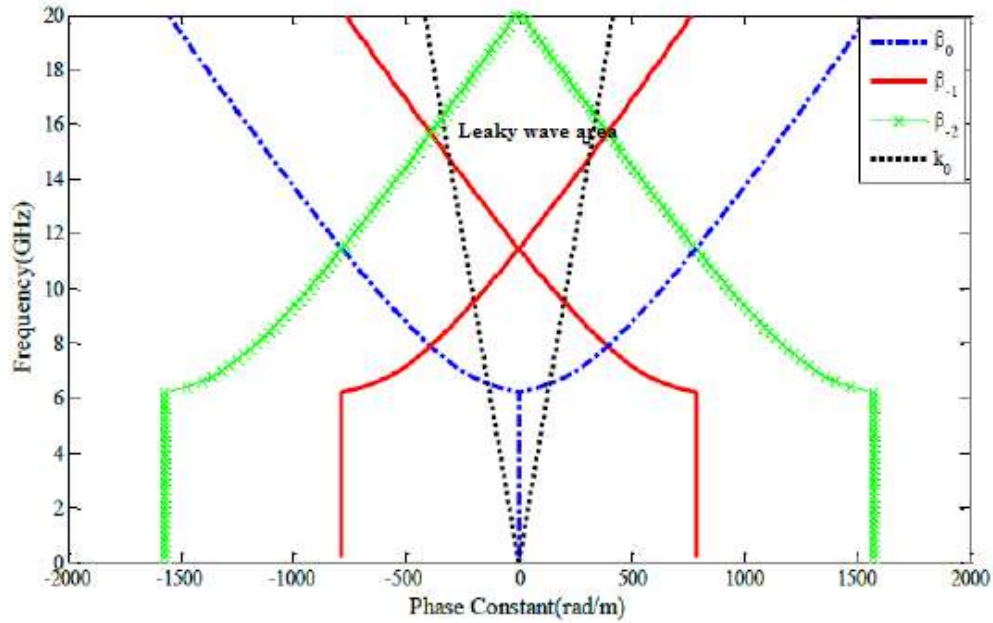
$$\beta_m = \pm\sqrt{k_0^2\varepsilon_r\mu_\perp - (\frac{m\pi}{w_{off}})} \qquad m = 1, 2, 3, ... \qquad (2\text{-}37)$$

In the proposed structure, the structure should be designed so that $\beta_{-1} = 0$ occurs at a frequency of F=10.2 GHz (the beginning of the leakage wave region is at this frequency). By using equation (2-34) and unit cell length p=8.2 mm, we have:

$$\beta_{-1} = \beta_0 - \frac{2\pi}{p}|_{f=10.2\ GHz} = 0 \ \rightarrow \beta_0$$

$$= \sqrt{(2\pi f)^2\varepsilon\mu - \left(\frac{\pi}{w_{off}}\right)^2} = \frac{2\pi}{p} \qquad (2\text{-}38)$$

By solving the above equation, the wavelength width is obtained $w_{off} = 9.4\ mm$ (However, this value is an approximate width, and the optimal effective width of this structure is 9.55 mm).

The scattering curve for the predominant rectangular waveguide mode, TE_{10}, is plotted in Figure 2-17.

Figure 2-17: Scattering curve of a periodic structure based on a rectangular waveguide in the dominant mode

It should be noted that in this curve, the phase constant is related to the waveguide and the disturbance (finger gap) is assumed negligible. In fact, this method is designed only to

approximately find the area of the leaky wave based on the overall dimensions of the structure and the characteristics of the substrate. The accurate area of the leaky wave is determined by simulating the whole wave and extracting the scattering curve.

2.4 Microstrip antenna

The concept of microstrip radiators was first introduced by Deschamps in late 1953 and the first practical antenna was developed in 1970. Since then, extensive research has been conducted on various microstrip antennas. A microstrip antenna in the simplest type of configuration, as shown in Figure 2-18, consists of an insulator with a dielectric constant of less than 10, with a ground plate on one side and a radiant plate on the other. Is located. The radiant conductor plate is generally made of gold and copper. These conductors can have different shapes, but usually shapes are used that are expected to perform well and can be easily analyzed. Different types of insulation, dielectric constant and tangent have different losses. Ideally in the case of antennas, the dielectric constant of insulation to increase scattering and emitting fields should be less than 2.5 [25].
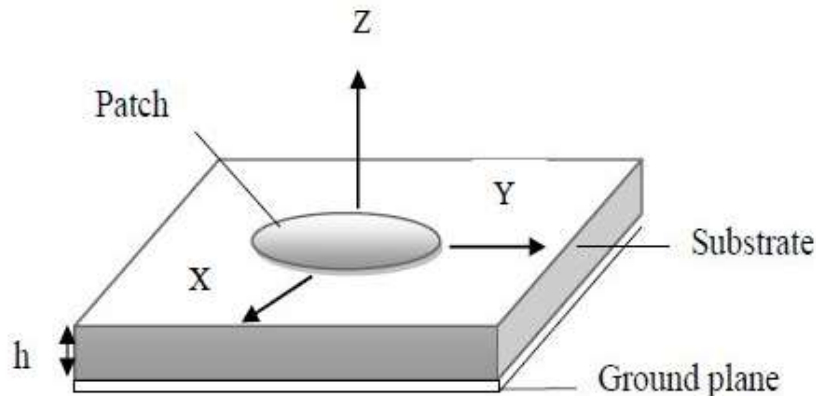

Figure 2-18: Microstrip antenna configuration [25]

2.4.1 Advantages and disadvantages of microstrip antennas

Microstrip antennas have several advantages over conventional microwave antennas, ranging from 100 MHz to 100 GHz, some of which include [25]:

- Having low weight and volume and low plate structure
- The possibility of manufacturing very cheaply for mass production
- Easy to build integrated with MICs on a substrate
- Possibility of linear or circular polarization with easy feeding methods
- Possibility of design for two-frequency and two-polarization modes
- Power supply lines and matching networks are made simultaneously with the antenna structure.

Despite these advantages, microstrip antennas have the following disadvantages:

- Narrow bandwidth and manufacturing error issues
- Less gain
- High ohmic losses in the feed structure of arrays

21

- Half screen radiation
- Having a complex feeding structure for arrays
- Poor polarization purity
- Sub-radiation from the power supply and connection points
- Stimulation of surface waves
- Poor power management capabilities

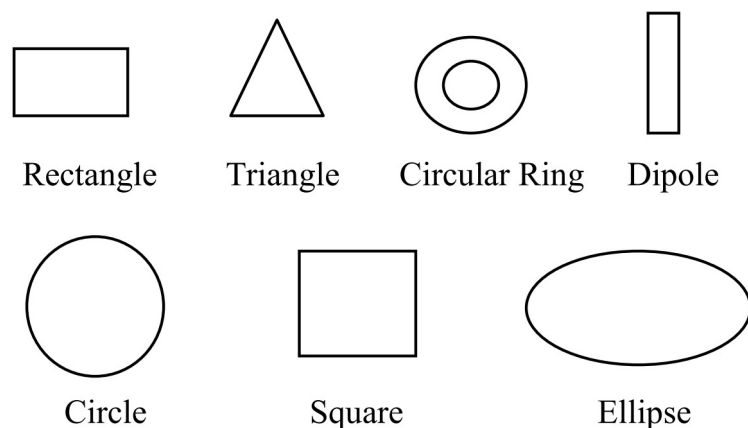## 2.4.2 Types of microstrip antennas

Microstrip antennas are described by a large number of physical parameters compared to conventional microwave antennas. These antennas have different types with their own characteristics and for applications. A variety are used according to the desired specifications. All microstrip antennas are divided into four main categories:

- 1.Microstrip patch antennas
- 2.Microstrip bipolar antennas
- 3.Microstrip slot antennas
- 4.Rising wave microstrip antennas

Microstrip antennas have a narrow bandwidth of 1 to 5% in normal mode, which is a major limiting criterion for the applications of these antennas. Most of the researchers' efforts in this category have been spent on increasing the bandwidth of this antenna and the bandwidth of up to 70% has been achieved [26], [27].

2.4.3 Microstrip patch antennas

These antennas consist of a flat or non-flat patch on one side of the dielectric and the ground plate on the other side of the dielectric. Patch thickness is generally considered [26]. There are many substrates used to design microstrip antennas, and their dielectric constants are usually in the range of 2.2 to 12. The height of the substrate in this antenna is. Low dielectric constants have higher efficiencies and higher bandwidth, which is associated with a larger underlayer height. Thin substrates with dielectric constants are more suitable for microwave circuits because they require limited fields to minimize adverse radiation but will have lower bandwidth and efficiency. The patch has different shapes. The most important ones that have practical applications and are mostly used in the design of antennas, shown in Figure 2-19

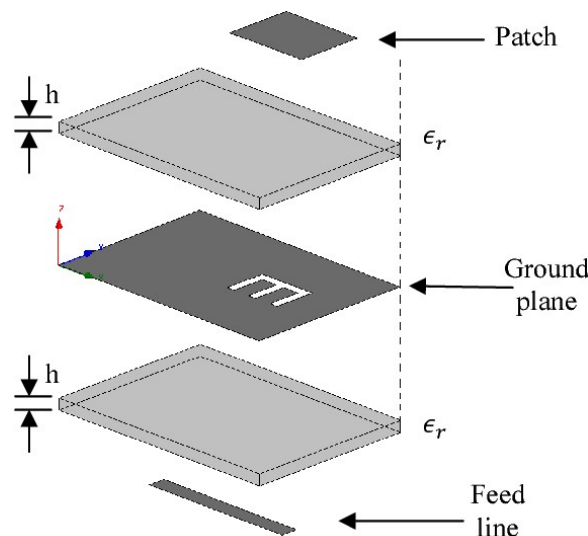| Rectangle | Triangle | Circular Ring | Dipole |

| Circle | Square | Ellipse |

Rectangular and circular patches are commonly used because they are easier to analyze and fabricate and have good radiative properties, especially since they have low cross-polarization radiation, and typically patch antennas with a gain of 5 to 6 dB and a width range. Its 3 dB beam is from 70 to 90 degrees.

2.4.4   Microstrip bipolar antennas

This type of antenna has a different length to width ratio in terms of shape compared to the patch. The width of bipolar antennas is usually less than 0.05. The radiation patterns of patch and bipolar antennas are the same due to their similar longitudinal current distribution, but their radiation resistance, bandwidth, and cross-polarization are very different [27]. So, they are suitable for arrays. These antennas are widely used in very high frequencies and for this purpose, their thick substrate (representing capacitors with far apart plates, reducing stored energy, and reducing the quality factor) is selected to obtain the appropriate bandwidth. The power supply network is very important for these antennas and should be considered in the analysis stage.

2.4.5   Microstrip slot antennas

In this type of antenna, a slot is located on the ground of a grounded substrate. Figure 2-20 shows the shape of this type of antenna. Power of this type of antenna is using microstrip lines or coplanar waveguides. These antennas are usually two-way radiators because they radiate on both sides of the slot. One-way radiation is obtained when a reflecting plate is placed on one side of the slot. Slot antennas have advantages over patch antennas. For example, they create more bandwidth, and basically with antennas, the antenna can be compressed as much as possible.
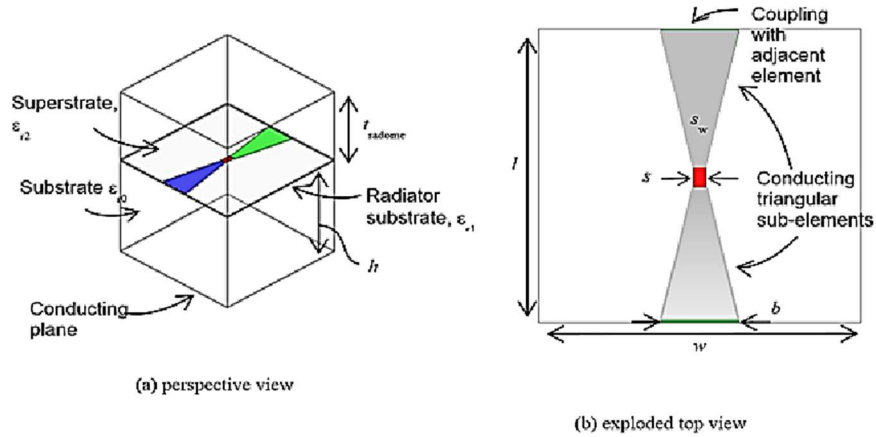

Figure 2-20: Microstrip slot antennas [26]

2.4.6   Traveling wave microstrip

These types of antennas have a series of alternating chain conductors or consist of a long microstrip line wide enough to establish a TE wave (Figure 2-21). These antennas are adapted by a resistive load to prevent the generation of standing waves. If the antenna system is designed

in such a way that the load connected to the end of the antenna has a high impedance matching with the whole previous system, then the generated wave is not returned by the source at the end of the antenna. In fact, this type of antenna is considered as a conductor of traveling waves. If the dimensions of the antenna are too large, then the power of the output waves of the source is scattered and wasted in this long distance, which as a result makes us have no power return. Then the current and voltage in the whole system will have similar problems. Therefore, the input impedance of these antennas is pure and real and in general, they produce high bandwidth. These antennas are designed so that their radiation pattern is at a distance between the radiation from the side and the radiation from the end.

(a) perspective view

(b) exploded top view

Figure 2-21: Traveling wave antennal [28]

Chapter 3

3 Arduino

Arduino is in fact a hardware and software platform for implementing a variety of electronic boards, the main purpose of which is to facilitate the construction and coding of boards and is available to the public in a completely open-source manner. By preparing many application modules as well as building a simple and streamlined coding platform, the Arduino eliminates the hassle of additional complexities such as initial setups and high wiring or writing all the basic functions required by hardware programming. Modules range from simple modules just for setting up the microcontroller to motor drive shields and even connecting to the Arduino Wi-Fi network are pre-designed and can be added to your projects. Coding for Arduino is also in Arduino, which is very similar to C ++, and can be compiled and programmed on the board in the Arduino compiler environment, and the very interesting thing about it is that many of the basic functions required in coding include Mathematical functions such as sine and ... or functions working with time and also functions with micro ancillary features such as Analog to digital converter or serial port, etc. in it with a lot of simplicity, even much easier to implement than an environment such as Code Vision This has been found to greatly reduce the convenience as well as the coding volume.

3.1 History of Arduino

Arduino project began at the Ivrea Interaction Design Institute in Ivrea, Italy. At that time, students used the BASIC Stamp microcontroller, which in those years imposed a significant cost on students. In 2003, Hernando Baragan created the Wiring Development Platform as a master thesis project in IDII under the direction of Massimo Banzi and Casey Rias (known for their work on the processing language)[29]. The goal of this project was to create simple and low-cost tools for digital projects created by non-engineers. The Wiring platform included a PCB with Atmega168 microcontroller, a Processing IDE, and library functions for easy microcontroller programming.

In 2003, Massimo Banzi, along with another IDII student, David Mellis, and David Quartill added support for the Atmega8 microcontroller to Wiring because it was cheaper. But instead of continuing to work on the Wiring, they split and renamed it Arduino. Early Arduino boards used a USB driver chip to FTDI serial and an Atmega168 microcontroller. Arduino Uno board with Atemga328P microcontroller and in older versions with Atmega16U2 microcontroller which is programmed as a USB to serial converter, was different from all previous boards [30].

3.2 Advantages and disadvantages of Arduino

In this section the advantages and disadvantages of Arduino device are listed [29]:

3.2.1 Advantages

➢ Very cheap: Arduino is incredibly cheaper than other microcontroller platforms.

> ➢ Comprehensive: Software used for Arduino programming (IDE) has the ability to run on Windows, Mac and Linux operating systems. While most microcontrollers can only be programmed in a Windows environment.
>
> ➢ Clear and simple programming environment: Although IDE software is very easy for beginners, it is also very flexible for professionals and programming professionals and can take full advantage of all its benefits. To take.
>
> ➢ Open source and extensible software: Arduino software has been published as open source so that professionals can work on it and develop it. This software can be developed by C ++ programming language and those who want to get more details can jump from Arduino to AVR-C programming language. Likewise, you can add the AVR-C code directly to your Arduino software if you wish.
>
> ➢ Expandable and open-source hardware: The Arduino chip is designed so that electronics, computer, etc. engineers can easily apply their desired changes to it.

3.2.2 Disadvantages

While the Arduino has many advantages, it also has a number of disadvantages.

> – It should be noted, however, that these disadvantages are due in large part to the inherent limitations of AVR controllers. For example, because the microcontroller connects to the USB port, the input and output pins on some boards will be shorter.
>
> – It takes up a lot of space. For example, if you use a microcontroller, you will need much less space. Also, if you are limited to using and programming Arduino, programming in other languages and other operating systems will be complicated for you due to the ease of Arduino programming.
>
> – It can be damaged if it is powered by high voltage. If you connect the Arduino Analog and digital pins to voltages above five, your board may be permanently damaged.

3.3 Applications of Arduino

Its Arduino chips are widely used. Here are some of the most common examples of its use:

- Different robots
- Queue counters in banks, parking lots and ...
- Phones and smartwatches
- Security systems of sensitive places
- Air conditioners that have sensors of temperature, humidity, etc. of the environment and regulate the amount of these variables.
- Advanced devices related to medical engineering

3.4 Different types of Arduino devices

In the following table, different types of Arduinos along with the details are listed.

Table 1: Arduino comparison table [31]

Boards	Microcontroller	Operating Voltage/s (v)	Digital I/O Pins	PWM Enabled Pins	Analog I/O Pins	DC per I/O (mA)	SRAM (KB)	Clock (MHz)	Length (mm)	Width (mm)	Cable
Uno	ATmega328	5	14	6	6	20	2	16	68.6	53.4	USB A-B
Leonardo	ATmega32u4	5	20	7	12	40	2.5	16	68.6	53.3	micro-USB
Micro	ATmega32u4	5	20	7	12	40	2.5	16	48	18	micro-USB
Nano	ATmega328	5	22	6	8	40	1	16	45	18	Mini_B USB
Mini	ATmega328	5	14		6	20	2	16	30	18	USB_Serial
Due	Atemel SAMX8E ARM Cortex M3 CPU	3.3	54	12	12	800	96	84	102	53.3	micro-USB
Mega	ATMega 2560	5	54	15	16	20	8	16	102	53.3	USB A-B
Mo	Atmel SAMD21	3.3	20	12	6	7	32	48	68.6	53.3	micro-USB
Yun Mini	ATmega32u4	3.3	20	7	12	40	2.5	400	71.1	23	micro-USB
Uno Ethernet	ATmega328p	5	20	4	6	20	2	16	68.6	53.4	Ethernet
Tian	Atmel SAMD21	5	20	12	0	7	64000	560	68.5	53	micro-USB
Mega ADK	ATMega 2560	5	54	15	16	40	8	16	102	53.3	USB A-B
M Pro	Atmel SAMD21	3.3	20	12	6	7	32	48	68.6	53.3	micro-USB
Industrial 101	ATmega32u4	5	7	2	4	40	64000	400	51	42	micro-USB
Uno Wifi	ATmega328	5	20	6	6	20	2	16	68.6	53.4	USB A-B
Leonardo Ethernet	ATmega32u4	5	20	7	12	40	2.5	16	68.6	53.3	USB A-B
MKR1000	Atmel SAMD21	3.3	8	12	7	7	32	48	64.6	25	micro-USB

According to the table above the Arduino Mega 2560 board is very versatile with more digital and Analog bases. In the continuation of the tutorial, we will introduce the Arduino Mega 2560 and examine its details.

3.5   Introducing the Arduino Mega 2560

The Arduino Mega 2560 board is a microcontroller board based on the ATMega 2560. This board has a total of 54 digital input / output pins, 15 of which can be used as PWM outputs, 16 Analog inputs, 4 UART ports (hardware serial ports), a 16 MHz crystal oscillator, a USB port, a power Jack, Has an ICSP Header and a reset button [31].

The Mega 2560 board includes all the features needed to use the microcontroller on the board. To get started, simply connect the board to your computer with just a USB cable, or run it with an AC-to-DC adapter or battery.

The Mega 2560 board is compatible with most shields designed for the Arduino Uno. Board / Arduino Mega 2560 replaces Arduino Mega

The Mega 2560 board is different from previous boards Because it does not use a USB-to-serial FTDI chip, and instead uses an ATmega16U2 or ATmega8U2 on the R1 and R2 version boards, which is programmed as a USB-to-serial converter.

Table 2: specifications of Arduino Mega 2560 [31]

Microcontroller	ATMega 2560
Operating voltage	5 V
Input voltage (recommended)	7-12 V
Input voltage (range)	6-20 V
Digital input / output pins	54, of which 13 pins can be used as PWM output
Analog input pins	16
DC current of each input / output pin	40 mA

DC current for 3.3V pin	50 mA
Flash memory	256 KB(8 KB is used by the bootloader
SRAM	8 KB
EEPROM	4 KB
Clock speed	16 MHz

3.5.1 Description of Arduino components

Each component of the board of Arduino Mega 2560 is described in Figure 3-1.

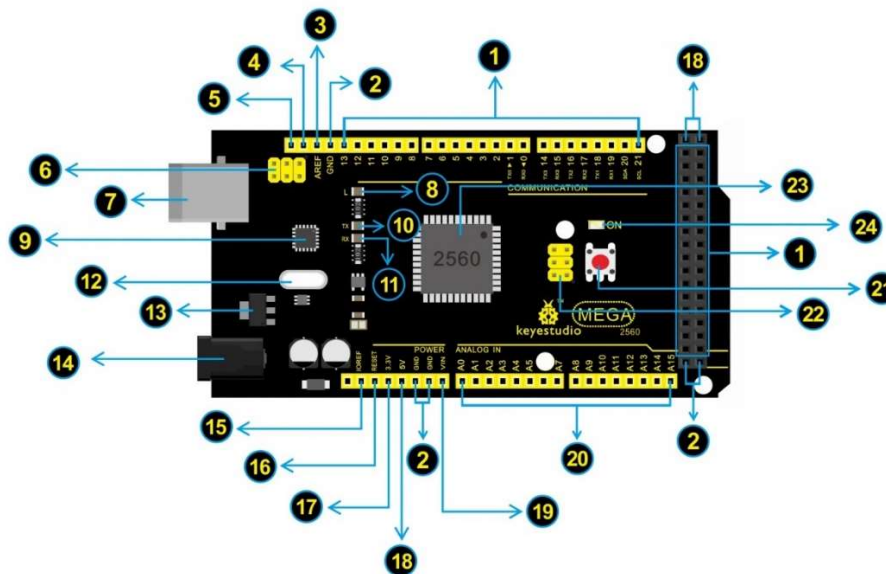Here is an explanation of what every element and interface of the board does:

Figure 3-1: Components of the board of Arduino Mega 2560 [32]

1- Digital I/O: Arduino MEGA has 54 digital input/output pins (of which 15 can be used as PWM outputs). These pins can be configured as digital input pin to read the logic value (0 or 1). Or used as digital output pin to drive different modules like LED, relay, etc. Using pinMode(), digitalWrite(), and digitalRead() functions.

2- GND: Ground pins

3- AREF: Reference voltage (0-5V) for analog inputs. Used with analogReference(). Configures the reference voltage used for analog input (i.e. the value used as the top of the input range).

4- SDA: IIC communication pin

5- SCL: IIC communication pin

6- ICSP (In-Circuit Serial Programming) Header: the AVR, an Arduino micro-program header consisting of MOSI, MISO, SCK, RESET, VCC, and GND. Connected to the ATMEGA16U2-MU. When connecting to PC, program the firmware to ATMEGA16U2-MU.

7- USB Connection: Arduino board can be powered via USB connector. All you needed to do is connecting the USB port to PC using a USB cable.

8- D13 LED: There is a built-in LED driven by digital pin 13. When the pin is HIGH value, the LED is on, when the pin is LOW, it's off.

9- ATMEGA 16U2-MU: USB to serial chip, can convert the USB signal into serial port signal.

10- TX LED: On-board you can find the label: TX (transmit). When Arduino board communicates via serial port, send the message, TX led flashes.

11- RX LED: on-board you can find the label: RX(receive).When Arduino board communicates via serial port, receive the message, RX led flashes.

12- Crystal Oscillator: How does Arduino calculate time? by using a crystal oscillator. The number printed on the top of the Arduino crystal is 16.000H9H. It tells us that the frequency is 16,000,000 Hertz or 16MHz.

13- Voltage Regulator: To control the voltage provided to the Arduino board, as well as to stabilize the DC voltage used by the processor and other components. Convert an external input DC7-12V voltage into DC 5V, then switch DC 5V to the processor and other components.

14- DC Power Jack: Arduino board can be supplied with an external power DC7-12V from the DC power jack.

15- IOREF: This pin on the board provides the voltage reference with which the microcontroller operates. A properly configured shield can read the IOREF pin voltage and select the appropriate power source or enable voltage translators on the outputs for working with the 5V or 3.3V.

16- RESET Header: Connect an external button to reset the board. The function is the same as reset button.

17- Power Pin 3V3: A 3.3 volt supply generated by the on-board regulator. Maximum current draw is 50 mA.

18- Power Pin 5V: Provides 5V output voltage

19- Vin: You can supply an external power input DC7-12V through this pin to Arduino board.

20- Analog Pins: on-board has 16 analog inputs, labelled A0 to A15.

21- RESET Button: You can reset your Arduino board, for example, start the program from the initial status. You can use the RESET button.

22- ICSP (In-Circuit Serial Programming) Header: the AVR, an Arduino micro-program header consisting of MOSI, MISO, SCK, RESET, VCC, and GND. It is often called the SPI (serial peripheral interface) and can be considered an "extension" of the output. In fact, slave the output devices to the SPI bus host. When connecting to PC, program the firmware to ATMEGA 2560-16AU.

23- Microcontroller: Each Arduino board has its own microcontroller. You can regard it as the brain of your board. The main IC (integrated circuit) on the Arduino is slightly different from the panel pair. Microcontrollers are usually from ATMEL. Before you load a new program on the Arduino IDE, you must know what IC is on your board. This information can be checked at the top of IC.

24- Power LED Indicator: Powering the Arduino, LED on means that your circuit board is correctly powered on. If LED is off, connection is wrong.

3.6 Setup and Configure Arduino Hardware to MATLAB

To connect Arduino boards with MATLAB software, you must install backup packages for Arduino boards in this software. By installing these backup packages, Arduino boards communicate directly with MATLAB and Simulink software, and we can apply any control system we design in this software directly to these boards. Now we will introduce MATLAB software backup packages for Arduino boards and have an overview of their features and how they work. To connect Arduino boards with MATLAB software, you need to install backup packages for Arduino boards in this software. By installing these backup packages, Arduino boards communicate directly with MATLAB and Simulink software, and we can apply any control system we design in this software directly to these boards. We now introduce MATLAB software backup packages for Arduino boards and have an overview of their features and how they work

MATLAB software support packages for Arduino boards are provided in two separate packages [33]:

➢ MATLAB software backup package for Arduino board: Used to connect the Arduino board to MATLAB software
➢ Simulink software backup package for Arduino board: Used to connect Arduino board with Simulink software

3.7 MATLAB software backup package for Arduino board

The MATLAB support package for Arduino allows data to be read and written to the Arduino board and its connected devices such as Arduino motor shield, I2C device, and SPI device. Since MATLAB is a high-level interpretive language, programming with it is easier than C ++ C + C and other compiled languages, and results can be viewed instantly from input / output instructions without compilation. MATLAB includes thousands of math, engineering, and graphing functions that can be used to analyze and visualize data collected from Arduino. The advantages of using MATLAB for Arduino programming are:

- Sensor information is read and written interactively without waiting for code to be compiled
- Sensor data analysis using thousands of pre-built functions for signal processing, machine learning, mathematical modelling and more
- Mapping data using the extensive features of MATLAB software
- Get information about Analog and digital sensors from the Arduino board
- Control other devices with digital and PWM outputs
- Starts DC motor, servo motor and stepper motor also support Adafruit Motor Shield
- Access to peripherals and sensors connected to I2C or SPI
- Connect to the Arduino board using a USB cable or wirelessly via Wi-Fi

3.8 Simulink software backup package for Arduino board

Using the Simulink backup package for Arduino boards, Simulink can be used to develop and

simulate algorithms that run independently on Arduino. This package includes [33]:

➢ Detect hardware plug-in for Arduino board in MATLAB and installation pages for initial configuration of Arduino board
➢ Simulink blocks for configuring and accessing Arduino inputs and outputs
➢ External mode for setting interactive parameters and monitoring signals for algorithms running on the device
➢ Independent implementation of the model on the Arduino board (Standalone)
➢ Simulink access to input / output of accessories connected to the Arduino board before using models on hardware, including digital inputs and outputs, i2c read and write, SPI read and write, Analog inputs and outputs, as well as width modulation pulse (Simulink IO)

More detail about the configuration of Arduino hardware in MATLAB are described in Appendix A.

Chapter 4

4 Results

4.1 Scenario #1

In this scenario, considering following commands in MATLAB, a LED will be turn on.

In this project, we connect an LED to Pin 13 in Arduino as follows.

Figure 4-1: A LED connected to pin 13

Then we turned on the LED with the command you see in the following figure;

Figure 4-2: Turn on LED connected to pin 13

Figure 4-3: Led is turned on

Then we can turn off the LED with the active command you see in image.

Figure 4-4: Turn off LED connected to pin 13

More detail about the process of implementation of this scenario are provided in **Appendix A. Convert Simulink model to Arduino code.**

4.2 Scenario #2

In this scenario we want to turn on 12 LEDs simultaneity. In this code we use digital port of Arduino from 2_13 and also, we should use command "For" that we can build command "WriteDigitalPin" for each LED.

we turned on the LEDs with the following command.

Figure 4-5: turn on 12 LEDs
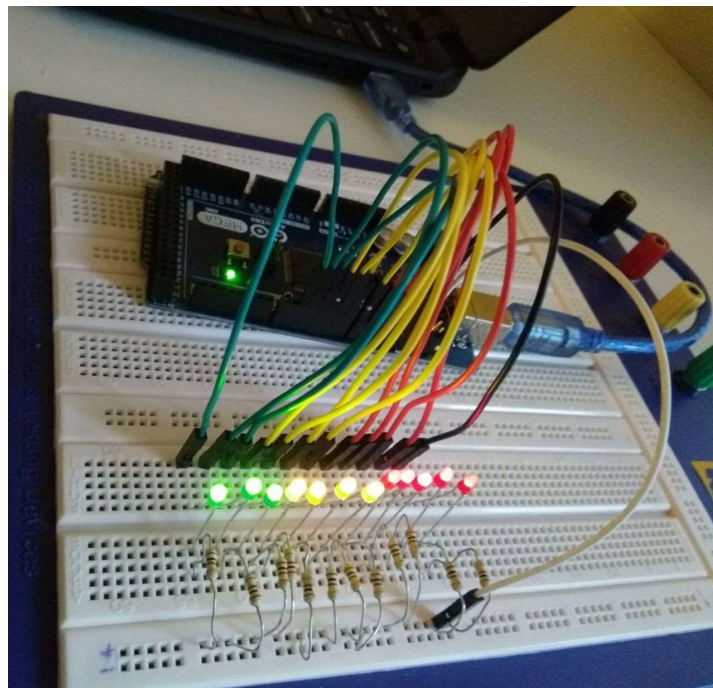
In the following figure, all 12 LEDs are switched ON.

Figure 4-6: All 12 LEDs are switched ON

4.3 Scenario #3

In the following command, a LED is switched ON and OFF at the same time

```
     Editor - E:\master_thesis\simulink\Test4.m
      Test4.m  ×  +
 1
 2 -    clc
 3 -    clear all;close all;
 4 -    MyArduino = arduino()
 5
 6 -  ☐  for ii=2:13
 7
 8 -       H2='D'
 9 -       LED=strcat(H2,num2str(ii));
10 -       eval('LED')
11
12 -       writeDigitalPin(MyArduino,LED,1);
13
14 -     └ end
15 -  ☐  for ii=2:13
16
17 -       H2='D'
18 -       LED=strcat(H2,num2str(ii));
19 -       eval('LED')
20
21 -       writeDigitalPin(MyArduino,LED,0);
22
23 -     └ end
```

Figure 4-7: LED Switch ON, then OFF

4.4 Scenario #4

In this part LEDs are switched ON by sequence.

```
     Editor - E:\master_thesis\simulink\Test5.m*
      Test5.m*  ×  +
 2 -    clear all;close all;
 3 -    MyArduino = arduino()
 4
 5 -    cmd_string_1=[0 1 1 1 1 1 1 1 1 1 1 1]
 6 -    cmd_string_2=[0 0 1 0 1 0 1 0 1 0 1 1]
 7 -    cmd_string_3=[0 0 0 0 0 0 0 0 0 0 0 0]
 8 -    cmd_string_4=[0 1 0 1 0 1 0 1 0 1 0 1 0]
 9 -    cmd_string=cmd_string_2
10 -  ☐ for ii=2:13
11
12 -    H2='D'
13 -    LED=strcat(H2,num2str(ii));
14 -    eval('LED')
15 -    led_val=eval(num2str(cmd_string(ii)))
16 -    writeDigitalPin(MyArduino,LED,led_val);
17 -   └ end
18 -    cmd_string=cmd_string_4
19 -  ☐ for ii=2:13
20
21 -    H2='D'
22 -    LED=strcat(H2,num2str(ii));
23 -    eval('LED')
24 -    led_val=eval(num2str(cmd_string(ii)))
25 -    writeDigitalPin(MyArduino,LED,led_val);
26 -   └ end
```

Figure 4-8: LEDs switch ON by sequence

4.5 Scenario #5

In this scenario we want to use one button to read the digital input from it and pay attention to its status and turn the digital output on and off according to the situation.

To do this, we have an LED and a push button, and we want our LED to turn on or off every time we press the pushbutton. we connect the push button to the digital pin 2 and the LEDs to

35

the digital pins 3 to 12 on the Arduino board.

We create a permanent loop "True" in which we read the values of the pressure key and their position and find out what position they are in.

Inside "while" we define a variable called "keystate "that reads and stores the position of the push key using the command "readDigitalPin".

Using the "writeDigitalPin "position, we apply the" keystate " position on the LED (in this project LED on = 0&LED off = 1) and using the "disp" to show the status of "key state".

```matlab
Pushbutton_LEDs.m   ×   +

2       function[] = Pushbutton_LEDs()
3  -     MyArduino = arduino()
4
5  -     PB  = 'D2';
6  -     finishup = onCleanup(@() ExitProgram(MyArduino));
7  -     disp('For Exit Program Press Ctrl+C');
8
9  -     while 1
10 -         for ii=3:13
11 -           H2='D'
12 -           LED=strcat(H2,num2str(ii));
13 -           eval('LED')
14 -           disp(LED)
15 -           keyState = readDigitalPin(MyArduino,PB);
16 -           writeDigitalPin(MyArduino,LED,keyState);
17 -           disp(['PushButton Status is ', num2str(keyState)]);
18 -         end
19 -     end
20
21 -     end
22
23       function ExitProgram(MyArduino)
24 -     clear MyArduino;
25 -     clear all;
26 -     disp('Program Terminated');
27 -     end
```

Figure 4-9: Turn on or off with pushbutton

```
Command Window
 D11
 PushButton Status is 0

 H2 =

     'D'


 LED =

     'D12'

 D12
 PushButton Status is 0

 H2 =

     'D'


 LED =

     'D13'

 D13
fx
```
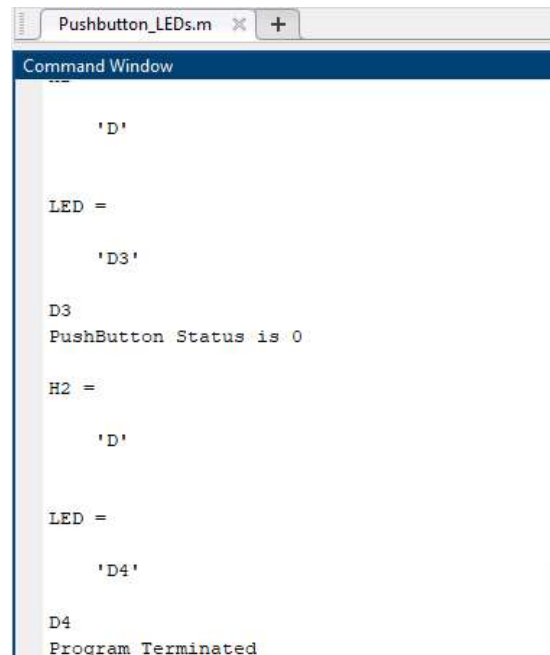
Figure 4-10: push button value

And to stop the program process, we use the key "Control + C " .

Figure 4-11: stop the process of the program

We learned from this section that we read the digital input of values and apply the same value to the digital output.

4.6 Scenario #6

In this scenario, we intend to create a square wave on one of the Arduino pins. The square wave or PWM is the same as disconnecting and connecting the voltages of 0 and 5 volts with a specified time interval. Then adjust the output of the Arduino pin by increasing or decreasing the wavelength.

First, we define"function "then we specify PWM with LED pins.

We create a loop "while "and inside it we write a command that the LED light goes up to the maximum value and then decreases.

To do this, we use a "For" and a voltage variable and give it a value.

```
while 1
    for ii=2:13
    H2='D'
    LED=strcat(H2,num2str(ii));
    eval('LED')%disp(LED)
     for voltage =0.0 : 0.5 :5.0
     writePWMVoltage ( MyArduino,LED,voltage);
     disp(['LED PWM is=',num2str(voltage)]);
     pause(0.5)
     end
     for voltage =5.0 : -0.5 :0.0
     writePWMVoltage ( MyArduino,LED,voltage);
     disp(['LED PWM is=',num2str(voltage)]);
     pause(0.5)
     end
    end
```

Figure 4-12: For iteration

We increase or decrease the voltage level by changing the "Duty Cycle" in "PWM".

By changing the pulse width, we created a variable voltage, so the larger the pulse width "Duty Cycle" the more voltage we applied.

Now, because the Arduino works from zero to 5 volts, and in this logic, when we have a 100% "Duty Cycle", it means that we have a maximum of 5 volts in it, and if we have a "Duty Cycle" of 0, the voltage becomes zero. In fact, whatever the duty cycle changes, practically the voltage changes.

Stop the process as much as you want with the "pause "command.

After running the program, we realize that our voltage is high and then decreases, as shown in the figure below

```
LED =

    'D12'

LED PWM is=0
LED PWM is=0.5
LED PWM is=1
LED PWM is=1.5
LED PWM is=2
LED PWM is=2.5
LED PWM is=3
LED PWM is=3.5
LED PWM is=4
LED PWM is=4.5
LED PWM is=5
LED PWM is=5
LED PWM is=4.5
LED PWM is=4
LED PWM is=3.5
LED PWM is=3
LED PWM is=2.5
LED PWM is=2
```

Figure 4-13: Voltages are changing

```
V_LEDs.m  ×  +
2    function[] = PWM_LED
3 -      MyArduino = arduino()
4 -      finishup = onCleanup(@()exitprogram(MyArduino));
5 -      disp ('for Exit Program Press Ctrl=C')
6 -   while 1
7 -          for ii=2:13
8 -          H2='D'
9 -          LED=strcat(H2,num2str(ii));
10 -         eval('LED')%disp(LED)
11 -          for voltage =0.0 : 0.5 :5.0
12 -          writePWMVoltage ( MyArduino,LED,voltage);
13 -          disp(['LED PWM is=',num2str(voltage)]);
14 -          pause(0.5)
15 -          end
16 -          for voltage =5.0 : -0.5 :0.0
17 -          writePWMVoltage ( MyArduino,LED,voltage);
18 -          disp(['LED PWM is=',num2str(voltage)]);
19 -          pause(0.5)
20 -          end
21 -          end
22 -   end
23 -   end
24    function exitprogram(MyArduino)
25 -      clear MyArduino;
26 -      clear all;
27 -      disp('Program has Exit')
```

Figure 4-14: Create square wave on the Arduino pins

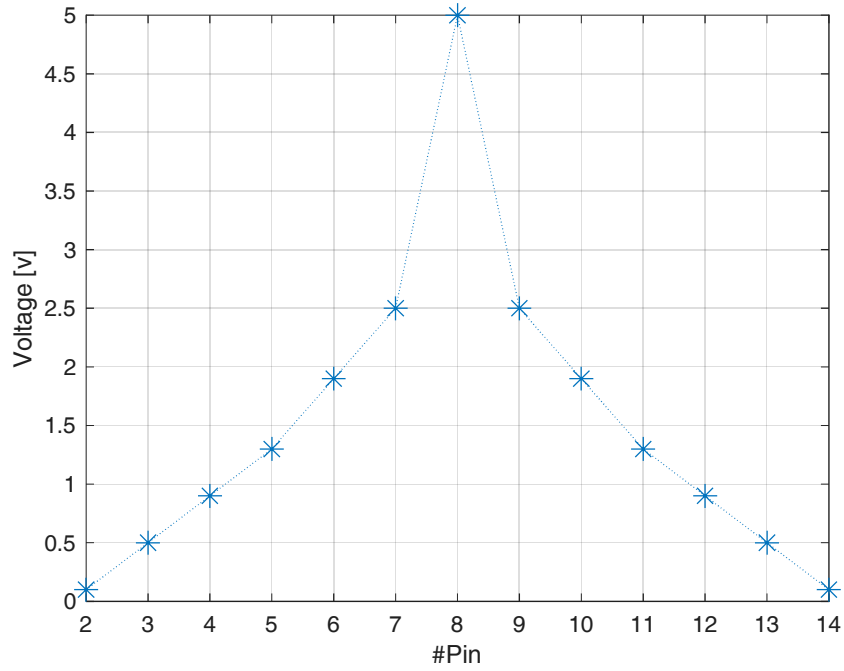If we want to change the voltage with different value we can use the blew code:

```matlab
function[] = PWM_LED
MyArduino = arduino()
finishup = onCleanup(@()exitprogram(MyArduino));
disp ('for Exit Program Press Ctrl=C')
cmd_string_2=[0 0.1 0.5 0.9 1.3 1.9 2.5 5 2.5 1.9 1.3 0.9 0.5 0.1];
figure(1)
X=2:14;
 plot(X,cmd_string_2(:,2:end))
 xlabel('#Pin');
 ylabel('Voltage [v]');
 xlim([2 14]);
 set(gca, 'XTick',X)
 grid on
cmd_string_3=[0 0.5 0.9 1.3 1.9 2.5 5 2.5 1.9 1.3 0.9 0.5 0.1 0.5];
figure(2)
X=2:14;
 plot(X,cmd_string_3(:,2:end))
 xlabel('#Pin');
 ylabel('Voltage [v]');
 xlim([2 14]);
 set(gca, 'XTick',X)
 grid on
z_string=zeros(size(cmd_string_3,2));
 while 1

    for ii=2:13
       H2='D'
       LED=strcat(H2,num2str(ii));
       eval('LED')%disp(LED)
       writePWMVoltage ( MyArduino,LED,cmd_string_2(1,ii));
        disp(['LED PWM is=',num2str(cmd_string_2(1,ii))]);
        pause(0.5)
        if ii==13
            for id=2:13
                H2='D'
                 LED=strcat(H2,num2str(id));
                eval('LED')%disp(LED)
                  writePWMVoltage ( MyArduino,LED,cmd_string_3(1,ii));
                 disp(['LED PWM is=',num2str(cmd_string_3(1,ii))]);
                  pause(0.5)
            end
```
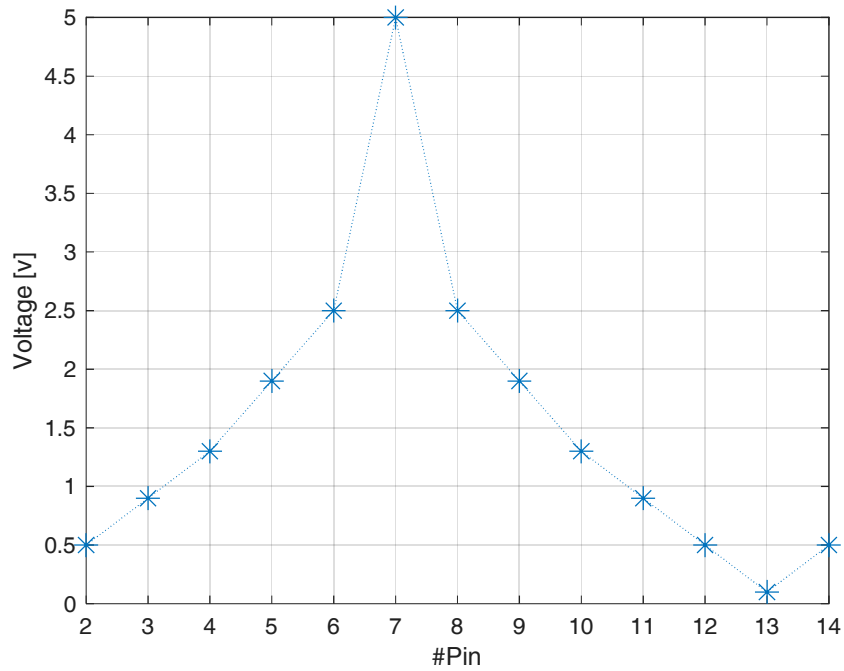
Figure 4-15: Imposing voltage variation by sequence

The results are shown as the following plots:

40

Figure 4-16: First random sequence; command string_2

Figure 4-17: Second random sequence; command string_3

As can be seen in the mentioned figures, by changing the sequence, the impact on the voltage of the diodes is observable.

4.7   Scenario #7

In this section, we want to show time modulated periodic structure by changing the voltage with LEDs. we have fixed periodicity and after that we want to change the periodicity

dynamically. we can change LEDs with sinusoidal shape.

The circular shift command in MATLAB is used to create a circular shift in the rows or columns of a matrix, or both.

Circularly Shift Rows or columns of a matrix, for example, if we have a matrix with 3 rows, for a circular shift (circle shift). R - Circularly Shift) Its rows are 1 unit (1 positive unit), row 1 instead of row 2 and row 2 instead of row 3 and row 3 which is the last row of the matrix, instead Row number 1 (the first row of the matrix) is placed. In fact, each row moves forward one by one, and the rows that are the last row will come to the beginning of the matrix and will replace the first row of the matrix.

Circular Shift for Columns A matrix is similar to Row, except that it has a circular shift in the direction of the columns. (Column) will be (columns will be moved).

If we want to have 1 unit of circular shift (Circular Shift) for the rows of a matrix named A and store the result in a matrix named B, we can use the following command: *circshift*.
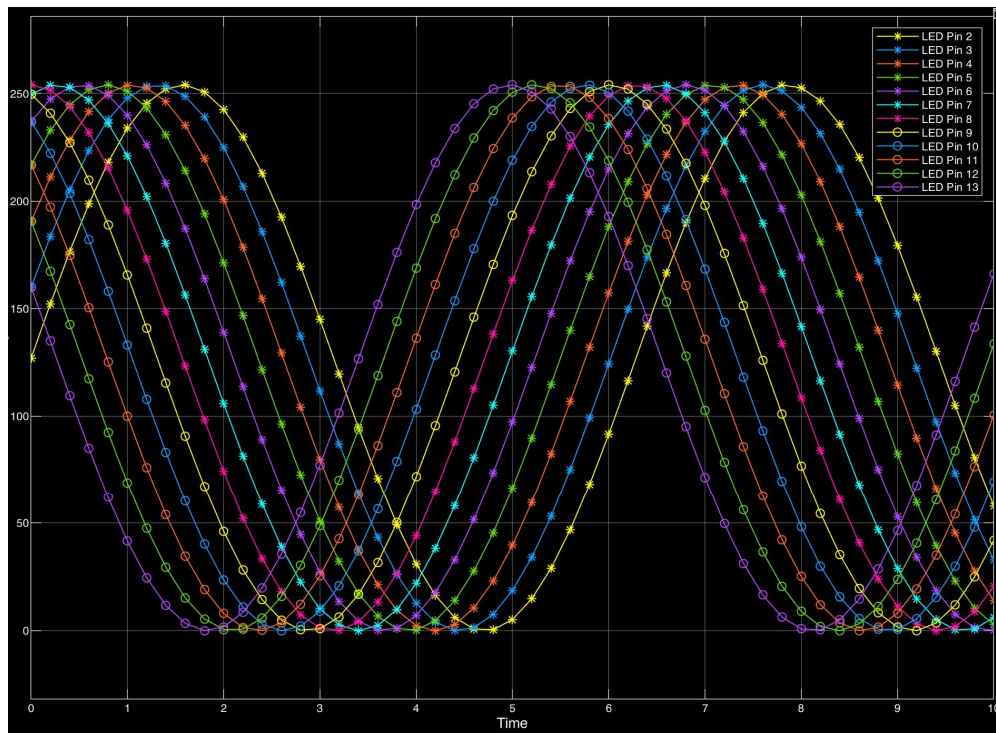
B = circshift(A,[1 0])

```matlab
1   function[] = shift_LEDs
2   MyArduino = arduino()
3   finishup = onCleanup(@()exitprogram(MyArduino));
4   disp ('for Exit Program Press Ctrl=C')
5   while 1
6       cmd_string_1=[0 0 1 0 1 0 1 0 1 0 1 0 1];
7       cmd_string=cmd_string_1
8       disp(cmd_string_1)
9       for ii=2:13
10          H2='D'
11          LED=strcat(H2,num2str(ii));
12          eval('LED')
13          led_val=eval(num2str(cmd_string(ii)))
14          writeDigitalPin( MyArduino,LED,led_val);
15          cmd_string_2=circshift(cmd_string_1,[0,1])
16          cmd_string=cmd_string_2
17          disp(cmd_string_2)
18      end
19      for ii=2:13
20          H2='D'
21          LED=strcat(H2,num2str(ii));
22          eval('LED')
23          led_val=eval(num2str(cmd_string(ii)))
24          writeDigitalPin( MyArduino,LED,led_val);
25          cmd_string_3=circshift(cmd_string_2,[0,1])
26          cmd_string=cmd_string_3
27          disp(cmd_string_3)
28      end
29
30      for ii=2:13
31          H2='D'
32          LED=strcat(H2,num2str(ii));
33          eval('LED')
34          led_val=eval(num2str(cmd_string(ii)))
35          writeDigitalPin( MyArduino,LED,led_val);
36          cmd_string_4=circshift(cmd_string_3,[0,1])
37          cmd_string=cmd_string_4
38          disp(cmd_string_4)
39      end
```

Figure 4-18: Shift the sequence of illumination

In the above code, unit 1 is for Circular Shift in the row and Unit 0 is for the Circular

Figure 4-19: Plot of shift the sequence of illumination

Chapter 5

5 Conclusion

In this thesis the Implementation of dynamic control of the change of the periodicity of a 24-bit long sequence by Arduino board are investigated.

In first chapter, a short introduction about the leaky wave antenna and tunable periodic structures was provided. A literature review, introduction and detailed information of leaky wave antennas described in the first part of chapter two. The rest of this chapter have been oriented to the introduction, definition, and formalization of metamaterials, substrate integrated waveguide, and microstrip antenna. The third chapter provided an introduction and application of different type Arduino. The advantages and disadvantages of the Arduino device presented in detail in the third chapter. Chapter four shows the results which have been simulated.
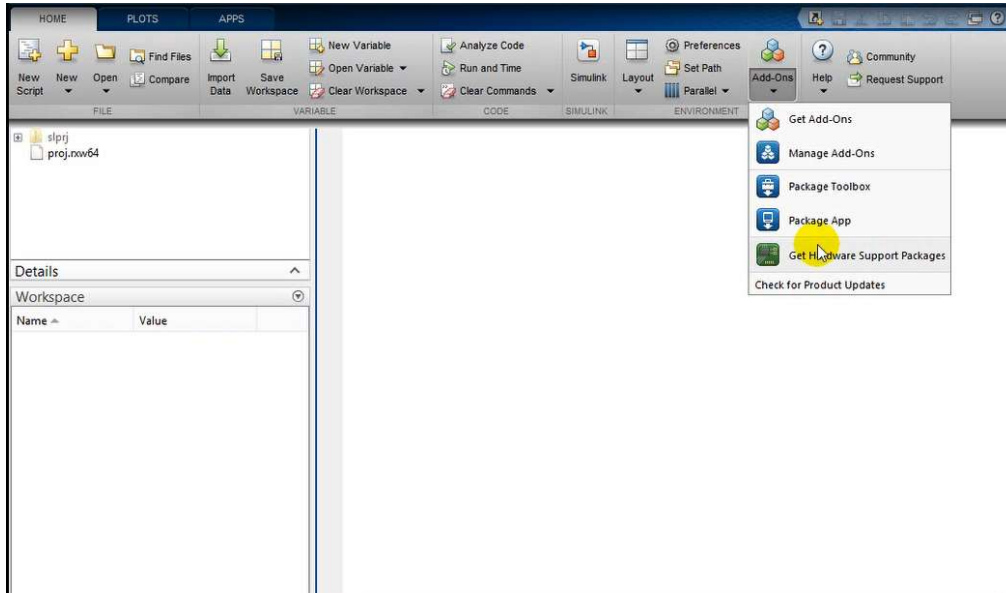
The model implemented in MATLAB environment. The experimental method verified by using Arduino hardware. Arduino Mega2560 was used to enable communication and control of connected diodes. All the proposed tuning scenarios are verified with Arduino board. By connecting the different LEDs to the designed bored and illuminating them, several scenarios have been checked.

By the experimental results obtained, the functionality of the developed code has been confirmed in the case of a time varying control signal. We can affirm that the presented experimental model can find application in time-modulated periodic structure.
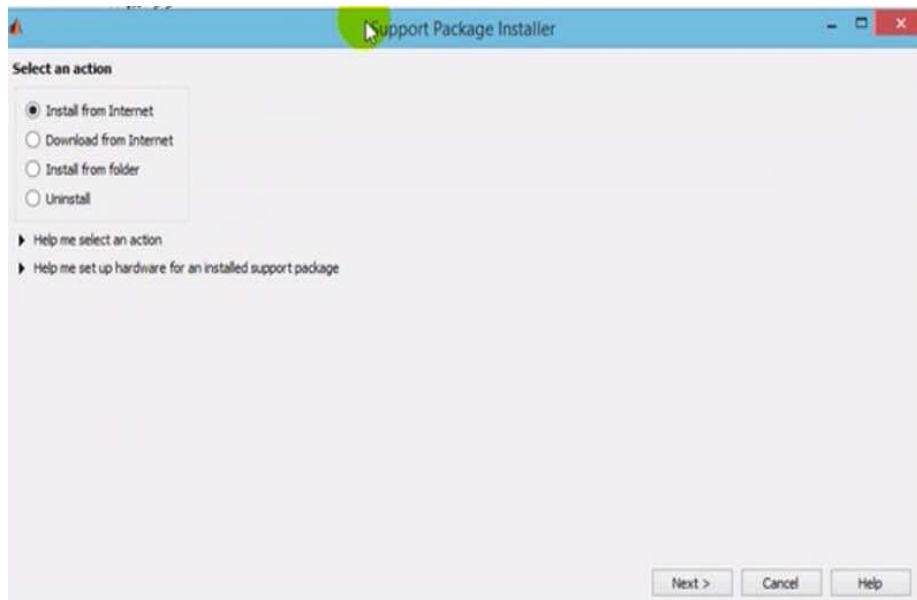
Appendix A

Installing Arduino package in MATLAB

The Arduino package is not installed by default in MATLAB software. You must first download and install this package. To do this, first enter the MATLAB software. Then click on Add one in the Home menu. Click Get hardware support packages as shown below.
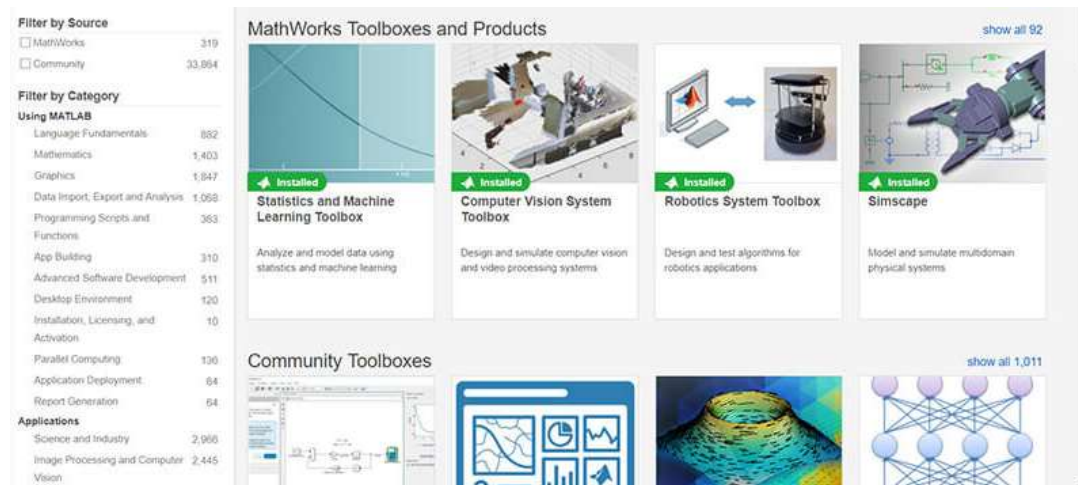

In the next step, the following window will open. This window may be different depending on the MATLAB software version.
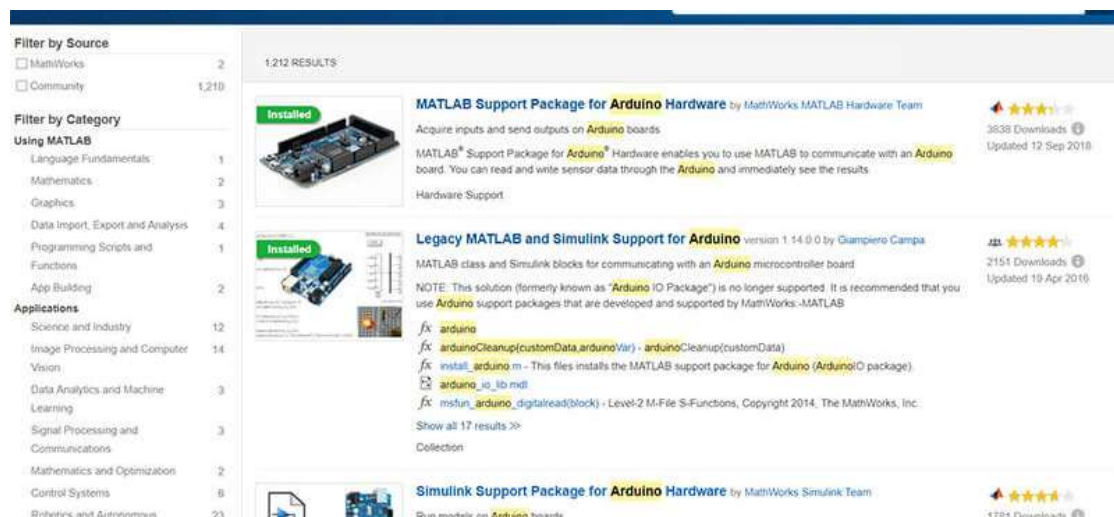

In the image above, the install from internet option directly downloads and installs the files from the MATLAB site. But if you choose to download from the Internet, it only downloads the files and you are responsible for installing it. Now select the install from internet option and click Next.

Then you can go to the package download step. At this point, a page like the one below will open.

Then by typing the phrase Arduino in the search field, you will see an image like the one below.

Click on the MATLAB Support Package for Arduino Hardware. After that, a window will open in which you must create an account on the MATLAB site to download these files. Click Create Account and create an account. After creating an account, click on Install, after downloading the files and installing them automatically by MATLAB software, you will be able to program Arduino.

After downloading and installing the packages by MATLAB software, connect the Arduino board to the computer.

we connect the Arduino board to the computer using a USB cable, as shown below

Display of bright LEDs on the board

After installing the program and connecting the board to the computer, the green light corresponding to the source marked with the PWR label should be lit (as in the picture above)

Arduino programming in MATLAB

To communicate with the Arduino board via MATLAB software; We have to assign an object to it, similar to object-oriented programming. Here, for example, we dedicate MyArduino to it. As you can see here, the board flashes and gives you this information.

You can see that MATLAB software detects which port and what type of board it is connected to. The available pins are also shown.

A few Arduino coding commands in MATLAB

```
a=arduino
```

Specifies the port number to which the Arduino connects and the type of Arduino board.

```
writeDigitalPin(1,2,3)
```

It is used to perform operations on a variable that is used as logic zero and one and includes the following:

1- The name you assigned to the existing board
2- The Pin number you want to operate on were
3- zero or one

```
pause();
```

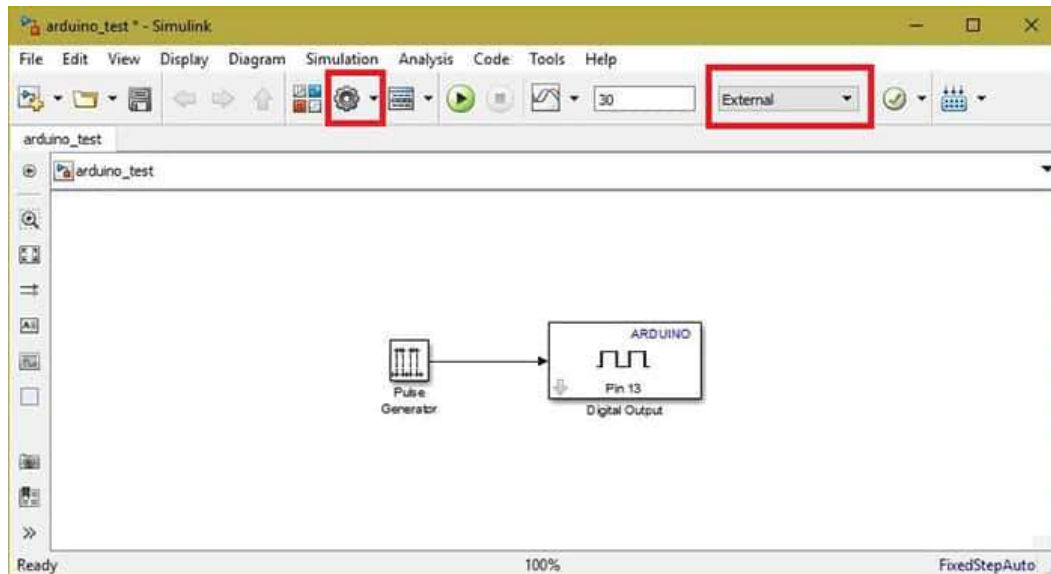The pause command is to stop the operation as much as desired and its unit is seconds.

Convert Simulink model to Arduino code

The interesting thing about MATLAB is that it has a large library of types of hardware, including specifications for each one, which makes it easier for you to think about coding for hardware. This means you can compile a MATLAB code for different hardware and upload it to them.
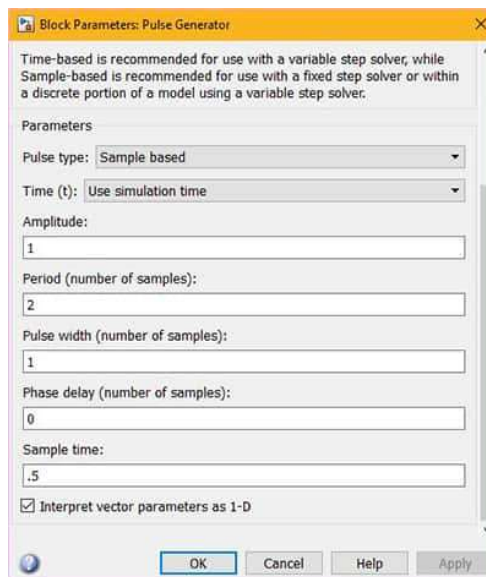
One of MATLAB's most efficient tools is Simulink. The main advantage of Simulink and its graphical environment is that the design of complex systems and the communication of their various components in this space is much easier than the coding environment. Arduino is also easier to connect to Simulink than MATLAB. When you enter Simulink you will see a new Arduino toolbox. This toolbox has various tools such as analog, digital and PWM communication along with tools for WiFi and Ethernet communication. You can design the most complex models of your software in Simulink and easily transfer it to Arduino, which is the first advantage of using this method. The second advantage of using Simulink with Arduino is the ability to easily convert your model to C ++/ C code and upload it directly to the Arduino board. In the Simulink window, set the run mode to External. Then click on the Model Configuration Parameters button to enter the Simulink settings. In the Hardware Implementation section, select your Arduino board.

I have prepared a simple program in Simulink that turns the Arduino LED on and off. To create this model, enter the **Pulse generator** block from the Sources section and the Digital output block from the Simulink support package for Arduino hardware section.
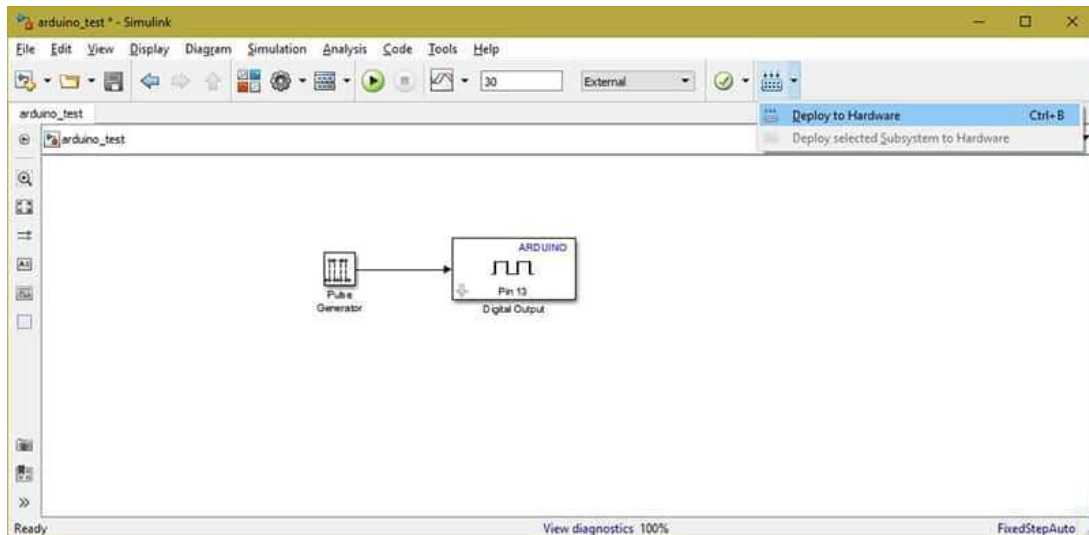
The digital output block, select "PIN 13" Open the **Pulse generator** block and select the **Sample based** value in the **Pulse type** field and the **Use simulation** time value in the **Time** field. Add other values that determine the flashing speed as shown below. You can change these values as you wish.

Now click on the **Deploy on hardware** button and wait for Simulink to generate your program code and load it on the Arduino. After completing the upload, you will see a message indicating that your application has been successfully compiled and uploaded. In fact, here we used Simulink instead of Arduino software to generate hardware code.
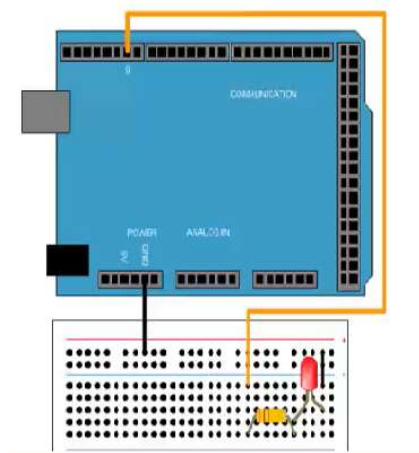
As before (we used MATLAB code) in Simulink you can delegate the processes to the computer and use Arduino as an interface. To do this, just click on the Run button instead of the Deploy key. In this case, like what we did with MATLAB, the computer will be responsible for processing and sending commands.

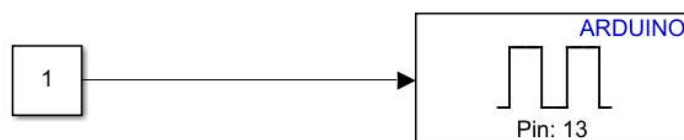We want to use ARDUION's digital outputs to turn on an LED.

To do this, we need several wires / one board / one resistor / one ((LED)) / one Arduino board. According to the figure below:

The shape of the circuit on the Arduino board

After that we connect board and run the program. we see the result that be like the first scenario.

The only difference with the previous case is that here with a feature called Pulse generator, we can have the LED flashing, and if we want it to have a zero or one mode, like scenario one, we have to use the constant capability, as shown in below Figure.

50

References

[1] C. H. Walter, *Traveling wave antennas*. New York: Dover Publications, 1970.

[2] F. Monticone and A. Alu, "Leaky-wave theory, techniques, and applications: from microwaves to visible frequencies," *Proc. IEEE*, vol. 103, no. 5, pp. 793–821, 2015.

[3] C. Caloz, D. R. Jackson, and T. Itoh, "Frontiers in antennas," *F. Gross, Ed. New York McGraw-Hill*, 2010.

[4] S. Lim, C. Caloz, and T. Itoh, "Metamaterial-based electronically controlled transmission-line structure as a novel leaky-wave antenna with tunable radiation angle and beamwidth," *IEEE Trans. Microw. Theory Tech.*, vol. 52, no. 12, pp. 2678–2690, 2004.

[5] T. Zvolensky, D. Chicherin, A. V Räisänen, and C. Simovski, "Leaky-wave antenna based on microelectromechanical systems-loaded microstrip line," *IET microwaves, antennas Propag.*, vol. 5, no. 3, pp. 357–363, 2011.

[6] Y. Geng, J. Wang, Y. Li, Z. Li, M. Chen, and Z. Zhang, "Leaky-wave antenna array with a power-recycling feeding network for radiation efficiency improvement," *IEEE Trans. Antennas Propag.*, vol. 65, no. 5, pp. 2689–2694, 2017.

[7] X.-C. Wang, W.-S. Zhao, J. Hu, and W.-Y. Yin, "Reconfigurable terahertz leaky-wave antenna using graphene-based high-impedance surface," *IEEE Trans. Nanotechnol.*, vol. 14, no. 1, pp. 62–69, 2014.

[8] Y.-L. Lyu, F.-Y. Meng, G.-H. Yang, D. Erni, Q. Wu, and K. Wu, "Periodic SIW leaky-wave antenna with large circularly polarized beam scanning range," *IEEE Antennas Wirel. Propag. Lett.*, vol. 16, pp. 2493–2496, 2017.

[9] S. S. Haghighi, A.-A. Heidari, and M. Movahhedi, "A three-band substrate integrated waveguide leaky-wave antenna based on composite right/left-handed structure," *IEEE Trans. Antennas Propag.*, vol. 63, no. 10, pp. 4578–4582, 2015.

[10] C. Caloz and T. Itoh, *Electromagnetic metamaterials: transmission line theory and microwave applications*. John Wiley & Sons, 2005.

[11] V. G. Veselago, "The Electrodynamics of Substances with Simultaneously Negative Values of Img Align= Absmiddle Alt= ϵ Eps/Img and μ," *Physics-Uspekhi*, vol. 10, no. 4, pp. 509–514, 1968.

[12] R. A. Shelby, D. R. Smith, and S. Schultz, "Experimental verification of a negative index of refraction," *Science (80-.).*, vol. 292, no. 5514, pp. 77–79, 2001.

[13] D. R. Smith, W. J. Padilla, D. C. Vier, S. C. Nemat-Nasser, and S. Schultz, "Composite medium with simultaneously negative permeability and permittivity," *Phys. Rev. Lett.*, vol. 84, no. 18, p. 4184, 2000.

[14] W. Zuo, Y. Yang, X. He, D. Zhan, and Q. Zhang, "A miniaturized metamaterial absorber for ultrahigh-frequency RFID system," *IEEE Antennas Wirel. Propag. Lett.*, vol. 16, pp. 329–332, 2016.

[15] A. Vélez, G. Sisó, A. Campo, M. Durán-Sindreu, J. Bonache, and F. Martín, "Dual-band microwave duplexer based on spiral resonators (SR) and complementary split ring resonators (CSRR)," *Appl. Phys. A*, vol. 103, no. 3, pp. 911–914, 2011.

[16] H. Lee, D.-J. Woo, and S. Nam, "Compact and bandwidth-enhanced asymmetric coplanar waveguide (ACPW) antenna using CRLH-TL and modified ground plane,"

IEEE Antennas Wirel. Propag. Lett., vol. 15, pp. 810–813, 2015.

[17]   A. Sanada, C. Caloz, and T. Itoh, "Novel zeroth-order resonance in composite right/left-handed transmission line resonators," in *Proc. Asia-Pacific Microwave Conf*, 2003, vol. 3, pp. 1588–1591.

[18]   J. Fu *et al.*, "An electrically controlled CRLH-inspired circularly polarized leaky-wave antenna," *IEEE Antennas Wirel. Propag. Lett.*, vol. 16, pp. 760–763, 2016.

[19]   K. Ichikawa, Z. Han, and H. Toshiyoshi, "Tunable terahertz bandpass filter using MEMS reconfigurable metamaterial," in *2017 International Conference on Optical MEMS and Nanophotonics (OMN)*, 2017, pp. 1–2.

[20]   W. Zhu, C. Wu, Q. Liu, and J. Du, "Frequency tunable metamaterials based on Ferroelectric substrate," in *2011 IEEE International Conference on Signal Processing, Communications and Computing (ICSPCC)*, 2011, pp. 1–4.

[21]   M. A. Abdalla and Z. Hu, "Compact metamaterial coplanar waveguide ferrite tunable resonator," *IET Microwaves, Antennas Propag.*, vol. 10, no. 4, pp. 406–412, 2016.

[22]   S. Adhikary, "Electric and Magnetic One-And Two-Dimensionally Tuned Parameter-Agile Substrate Integrated Waveguide Components and Devices." École Polytechnique de Montréal, 2014.

[23]   D. Deslandes and K. Wu, "Design consideration and performance analysis of substrate integrated waveguide components," in *2002 32nd European microwave conference*, 2002, pp. 1–4.

[24]   F. Xu and K. Wu, "Guided-wave and leakage characteristics of substrate integrated waveguide," *IEEE Trans. Microw. Theory Tech.*, vol. 53, no. 1, pp. 66–73, 2005.

[25]   R. Garg, P. Bhartia, I. J. Bahl, and A. Ittipiboon, *Microstrip antenna design handbook*. Artech house, 2001.

[26]   J. R. James, *Handbook of microstrip antennas*, vol. 1. IET, 1989.

[27]   K. F. Lee and W. Chen, *Advances in microstrip and printed antennas*. Wiley New York, 1997.

[28]   J. Liang, "Antenna study and design for ultra wideband communication applications." University of London United Kingdom, 2006.

[29]   E. Ramos, "Arduino basics," in *Arduino and Kinect Projects*, Springer, 2012, pp. 1–22.

[30]   M. Banzi and M. Shiloh, *Getting started with Arduino: the open source electronics prototyping platform*. Maker Media, Inc., 2014.

[31]   "Arduino." https://www.arduino.cc/en/Main (accessed Jan. 18, 2021).

[32]   A. Kurniawan, *Arduino Mega 2560 A Hands-On Guide for Beginner*. PE press, 2012.

[33]   "Matlab." https://in.mathworks.com/hardware-support/arduino-matlab.html (accessed Dec. 03, 2020).